NOTE TECHNIQUE

Reférence de la note	LNHB 2021/15

TITLE:

A BENCHMARK FOR MONTE CARLO SIMULATION IN GAMMA-RAY SPECTROMETRY

PART I: DETECTION EFFICIENCY

Authors:

M.C. Lépy, C. Thiam, M. Anagnostakis, R. Galea, D. Gurau, S. Hurtado, K. Karfopoulos, J. Liang, H. Liu, A. Luca, I. Mitsios, C. Potiriadis, M.I. Savva; T. T. Thanh, V. Thomas, R.W. Townson, T. Vasilopoulou, M. Zhang

ABSTRACT:

Monte Carlo (MC) simulation is widely used in gamma-ray spectrometry, however, its implementation is not always easy and can provide erroneous results. An exercise was organized in the frame of the Gamma-Ray Spectrometry Working Group (GSWG) of the International Committee for Radionuclide Metrology (ICRM) to provide a benchmark for several MC software used to compute the full energy peak efficiency and the total efficiency for selected detector-source cases. The examples are based on simple geometries, two types of germanium detectors and four kinds of sources, to mimic eight typical measurement conditions. The action outputs (input files and efficiency calculation results, including practical recommendations for new users) are made available on a dedicated webpage.

Key words:

Monte Carlo simulation, Gamma-ray spectrometry, Detector efficiency, EGSnrc, GEANT4, GESPECOR, MCNP, PENELOPE

CEA Saclay LIST-DM2I-LNHB 91191 Gif-sur-Yvette Cedex, France

A BENCHMARK FOR MONTE CARLO SIMULATION IN GAMMA-RAY SPECTROMETRY - PART I : DETECTION EFFICIENCY

M.C. Lépy[1], C. Thiam[1], M. Anagnostakis[2], R. Galea[3], D. Gurau[4], S. Hurtado[5], K. Karfopoulos[6], J. Liang[7], H. Liu[7], A. Luca[4], I. Mitsios[2], C. Potiriadis[6], M.I. Savva[8]; T. T. Thanh[9], V. Thomas[10], R.W. Townson[3], T. Vasilopoulou[8], M. Zhang[7]

1: CEA, LIST, Laboratoire National Henri Becquerel (LNE-LNHB), Bât. 602, PC 111, CEA-Saclay 91191 Gif-sur-Yvette Cedex, France
2: National Technical University of Athens, Nuclear Engineering Department, 15780, Athens, Greece
3: National Research Council of Canada, 1200 Montreal Rd., Ottawa, K1A 0R6 Canada
4: Horia Hulubei National Institute for R&D in Physics and Nuclear Engineering (IFIN-HH), 30 Reactorului street, PO Box MG-6, Magurele, Ilfov county, RO-077125
5: Universidad de Sevilla, Dpto. Física Aplicada II, ETSA, Avda. Reina Mercedes 2, 41012, Sevilla, Spain
6: Greek Atomic Energy Commission (EEAE), Environmental Radioactivity Monitoring Department, P.O. Box 60092, 153 10 Agia Paraskevi, Athens, Greece
7: National Institute of Metrology, Division of Ionizing Radiation, No.18, Bei San Huan Dong Lu, Chaoyang Dist, Beijing, Post Code: 100029, P.R.China
8: Institute of Nuclear & Radiological Sciences & Technology, Energy & Safety (INRASTES), NCSR "Demokritos", 15310, Ag. Paraskevi, Athens, Greece
9: University of Science, VNU-HCM, Faculty of Physics & Engineering Physics, Department of Nuclear Physics-Nuclear Engineering , 227, Nguyen Van Cu Street, Ward 4, District 5, Ho Chi Minh City, Viet Nam
10: CEA/DAM, France

Abstract:

Monte Carlo (MC) simulation is widely used in gamma-ray spectrometry, however, its implementation is not always easy and can provide erroneous results. An exercise was organized in the frame of the Gamma-Ray Spectrometry Working Group (GSWG) of the International Committee for Radionuclide Metrology (ICRM) to provide a benchmark for several MC software used to compute the full energy peak efficiency and the total efficiency for selected detector-source cases. The examples are based on simple geometries, two types of germanium detectors and four kinds of sources, to mimic eight typical measurement conditions. The action outputs (input files and efficiency calculation results, including practical recommendations for new users) are made available on a dedicated webpage.

Keywords: Monte Carlo simulation, Gamma-ray spectrometry, Detector efficiency, EGSnrc, GEANT4, GESPECOR, MCNP, PENELOPE,

Table of contents

1. Introduction

Monte Carlo simulation of radiation transport continues to grow in popularity in the fields of medical physics and radiation measurement, due in part to improvements of computation speed and to the modern usability of the codes. This concerns many different fields of application and, in the specific case of gamma-ray spectrometry, simulation is now commonly used to compute practical parameters which are used to quantify radioactivity in samples, such as the detection efficiency (Sima, 2012) and coincidence summing corrective factors (García-Toraño *et al.*, 2005).
Accurate efficiency calibration is required to perform optimisation procedures, by comparing the calculation results with experimental data in a large energy range, to validate the geometrical parameters used in the simulation model (Helmer *et al.*, 2004, Hurtado *et al.*, 2004, Peyres and García-Toraño, 2007).
Even if absolute detection efficiency values are difficult to calculate *ab-initio*, because of the lack of accuracy in the geometrical parameters of the detector, Monte Carlo simulation has been proved to be an efficient method to compute efficiency transfer factors as demonstrated by Vidmar *et al.* (2008).
Two kinds of Monte Carlo simulation software are used in gamma-ray spectrometry: these are either general multi-purpose codes (EGSnrc, GEANT4, MCNP, PENELOPE, etc.) or dedicated ones such as GESPECOR (Sima *et al.*, 2011), DETEFF (Cornejo Díaz and Jurado Vargas, 2008), etc. The dedicated codes are conceived with a user-friendly interface and can be directly applied to derive the calculation results from input data. On the contrary, the use of generalist codes needs some training in order to derive the information of interest. One of the typical difficulties is the preparation of the input files, which specify the geometrical conditions, since these must be written in a specific format.
This can be a challenge for new users who do not benefit from the advice of experienced users. Thus, in the framework of the Gamma-Ray Spectrometry Working Group (GSWG) of the International Committee for Radionuclide Metrology (ICRM), it was decided to provide some case studies and to prepare the corresponding input files for several codes, together with the expected results of the simulation. The action started in mid-2017 and the results were presented during the 22nd International Conference on Radionuclide Metrology and its Applications, in May 2019. The summary of the results has been published (Lépy *et al.*, 2020) and the present report includes the exhaustive series of results and comparisons obtained during the study.

2. Presentation of case studies

As training to use Monte Carlo (MC) simulation software, it was proposed to prepare geometrical files for a selection of high-purity germanium detectors (HPGe) and measurement conditions. In a first step, the exercise started with the simple models which were defined by Vidmar (2014) in an exercise dedicated to coincidence summing corrections. Geometry models include a detector and a source with different combinations; however, in all the cases, complete cylindrical symmetry of the arrangement of sample and detector is assumed.
Two kinds of coaxial high-purity germanium (HPGe) detector are considered. For both, the active crystal of the detector consists of a germanium cylinder with a thickness and diameter of 60 mm, with a 40-mm depth hole of 10 mm in diameter, with relative efficiency of about 20 %. It is installed in a 1-mm thick aluminium housing, with a length and diameter of 80 mm, and the crystal-to-window distance is 5 mm. The only difference between the two models is the dead layer thickness (on the top and side of the crystal), that is 1 mm or 0 mm to simulate either a p-type detector ("Detector A") or a n-type one

("Detector B"). In both cases, the housing diameter is the same as the window diameter. These dimensions are summarized in Table 1.

Table 1: Detector geometrical parameters. All dimensions are given in millimeters (mm)

Parameter	Detector A	Detector B
Crystal material	Ge	Ge
Crystal diameter (including the side dead layer)	60	60
Crystal length (including the top dead layer)	60	60
Dead layer thickness (top and side)	1	0
Hole diameter	10	10
Hole depth	40	40
Window diameter	80	80
Window thickness	1	1
Window material	Al	Al
Crystal-to-window distance	5	5
Housing length	80	80
Housing thickness	1	1
Housing material	Al	Al

One point source and three volume sources are considered, each located at 1 mm from the detector window. No source containers are to be simulated and the volume sources are cylinders made of water, silicon dioxide or cellulose with respective densities 1.0, 1.4 and 0.3 $g \cdot cm^{-3}$. The last two sample models are supposed to reproduce the measuring conditions of soils and filters. These sources are respectively denoted “P”, “W”, “S” and “F” in the exercise. The source parameters are presented in Table 2.

Table 2: Sample parameters. All dimensions are given in millimeters (mm)

Parameter	Water	Point	Soil	Filter
Sample diameter	90	-	60	80
Sample thickness	40	-	20	3
Sample material	Water	-	Dirt	Cellulose
Sample-to-window distance	1.0	1.0	1.0	1.0

Each source-detector assembly is installed in a 50-mm thick lead shielding, which has both a diameter and a height of 400 mm. The characteristics of various materials to be used in the simulation of the detector and sample models were also provided according to Vidmar (2014) and are shown in

Table 3.

Table 3: Characteristics of various detector and sample materials. All densities are given in g·cm^{-3}

Material	Density	Chemical formula
Ge	5.323	Ge
Al	2.70	Al
Water	1.0	H_2O
Dirt	1.4	SiO_2
Cellulose	0.3	$C_6H_{11}O_5$

Overall, eight configurations (2 detectors X 4 sources) were to be prepared; in this document, they will be referred to as identified in Table 4:

Table 4: Identification of the eight study cases

Name	Detector	Source
AP	A	Point
AW	A	Water
AS	A	Soil
AF	A	Filter
BP	B	Point
BW	B	Water
BS	B	Soil
BF	B	Filter

Figure 1 shows a schematic of the case of a point source and p-type detector (“AP” case); an example of the p-type detector in combination with the water source (without the external shielding) (“AW” case) is presented in Figure 2 and more details on the geometries are reported in ANNEX 1.

For each configuration, the participants were asked to prepare input files specific to the MC code they are familiar with, and to compute the full-energy peak efficiency (FEPE) and the total efficiency (TE) for five energies (50 keV, 100 keV, 200 keV, 500 keV and 1 MeV), for the eight combinations.

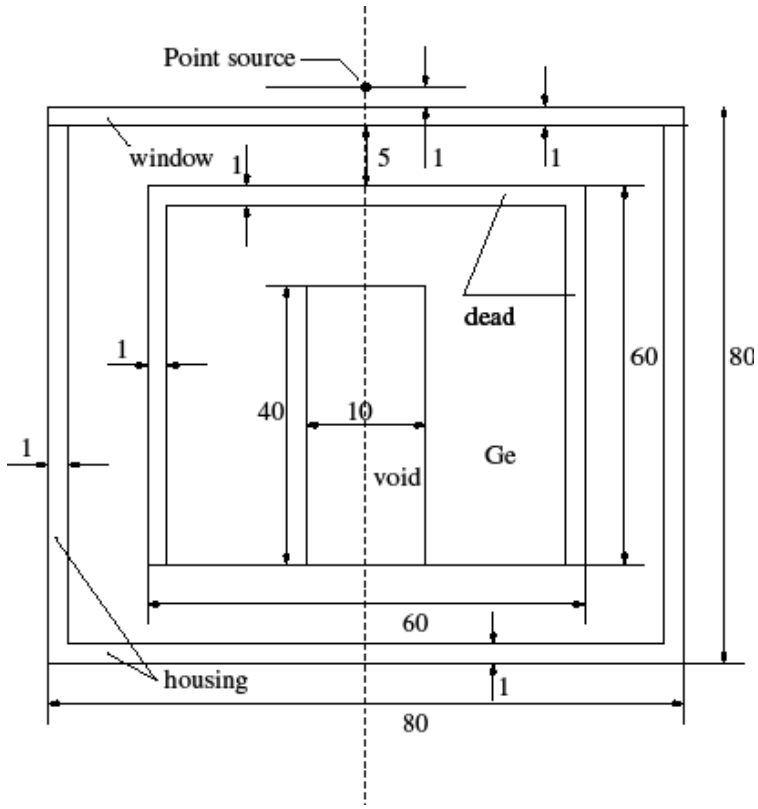

Figure 1: Schematic presentation of the model for the case of the point source and the p-type detector ("AP" case)

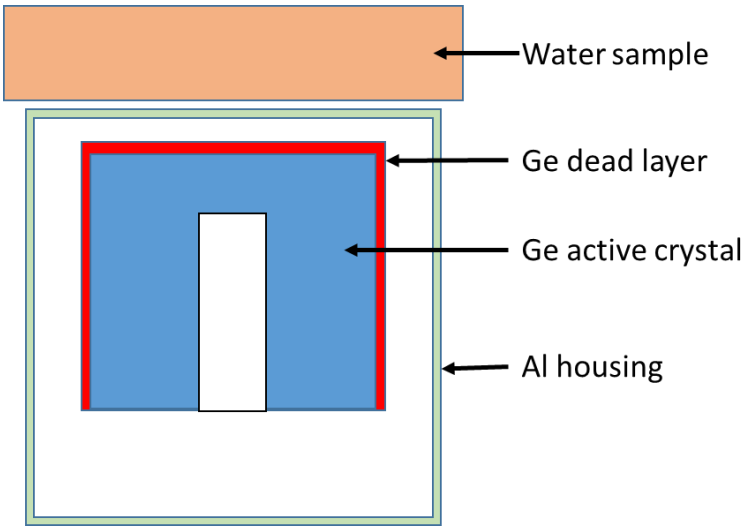

Figure 2: Geometrical model for the case of the water source and the p-type detector ("AW" case)

3. Short presentation of the Monte Carlo codes

In the present exercise, the participants used four general-purpose codes (EGSnrc, GEANT4, MCNP, PENELOPE) and one dedicated software (GESPECOR), and most of these have been used by several participants. Hereafter the general features of each code are summarized, mainly from the point of view of a "new user" for the practical use of Monte Carlo simulations. As each code requires specific input files to carry out the calculation, the participants in the action agreed on some common parameters and, if applicable, on the preparation of the calculation input files. A summary of the main parameters used in the simulations is presented in Table 1.

3.1 EGSnrc

EGSnrc (Electron Gamma Shower) (EGS, 2019) models the propagation of photons, electrons and positrons with kinetic energies between 1 keV and 10 GeV, in homogeneous materials. It is an open source software toolkit with applications in a range of radiation-related fields, particularly medical dosimetry. EGSnrc is an extended and improved version of the EGS4 code earlier developed (Nelson et al., 1985). The EGSnrc implementation improves the accuracy and precision of the charged particle transport mechanics and the atomic scattering cross-section data (Kawrakow, 2000), and includes a C++ class library for defining the geometry of complex simulation environments and particle sources. The core EGSnrc transport code remains in the MORTRAN language (Cook, 1983) which is an extended FORTRAN. For most applications, users can specify complex simulations using input files, without the need to write code. Visualization tools and GUIs are included.

3.2 GEANT4

GEANT4 (GEANT4, 2019) (GEometry ANd Tracking) is a general purpose Monte Carlo toolkit for the simulation of the passage and interaction of particles through matter, developed at CERN (Agostinelli *et al.*, 2003, Allison *et al.*, 2006, Allison *et al.*, 2016). It is written in C++ and exploits advanced software-engineering techniques and object-oriented technology. Its areas of application include high energy, nuclear and accelerator physics, as well as studies in medical and space science. GEANT4 offers a set of functionalities defined in specific C++ classes which users can call on to describe the different aspects of the experiment simulation (geometry, physical processes governing particle interactions, visualization of the detector and particle trajectories, data analysis at different levels of detail, etc.). However, the user must build his own application with three mandatory classes: *MyDetectorContruction* class, in which the geometry is defined in terms of volumes and filling materials physical properties; *ExpDetectorContruction* class, in which particles, interaction processes and physical models are specified through *ExpPhysicsList* class; and *ExpPrimaryGenerator* class in which the generation of primary particles is defined in *MyPrimaryGenerator* class. Optional classes can be added to manage the simulation stages as its progresses (*MyRunAction*, *MyEventAction* and *MySteppingAction*, etc.). A main program runs the simulation by calling in turn and bringing together the set of the basic and user GEANT4 classes.

3.3 GESPECOR

GESPECOR (Germanium SPectra CORrection) is a Monte Carlo based software, dedicated to gamma-ray spectrometry providing practical tools to perform the calculation of corrective factors (efficiency transfer, self-attenuation and coincidence summing corrections) and based on the methods developed by Sima et al. (2001). The computation routines are launched through a user-friendly interface, which can directly be applied to coaxial, planar or well-type high-purity germanium (HPGe) detectors with realistic dimensions including bulletized crystals, in a wide range of measurement configurations. Initially developed for the computation of the self-attenuation corrections and of the coincidence-summing corrections required to provide accurate quantitative results in gamma-ray spectrometry, the computation of the full energy peak efficiency and of the total efficiency was later added. Due to the optimization of the procedure, GESPECOR provides results in a relatively short time. Comparisons of the results obtained by GESPECOR and GEANT4 have been previously published (Chirosca *et al.*, 2013).

3.4 MCNP

MCNP6 (MCNP, 2019) is the latest version of the general-purpose Monte Carlo N-Particle code, developed at Los Alamos National Laboratory, that can be used for neutron, photon, electron, or coupled neutron/photon/electron transport (Briesmeister *et al.*, 2000, Goorley *et al.,* 2013). Specific areas of application include radiation protection and dosimetry, medical physics, nuclear criticality safety, etc. The code is written in FORTRAN and the user sets up simulations by creating a text file that is read by MCNP6. This input file has a dedicated structure and includes the geometry definition, and all the information needed for the radiation transport for the specific problem (source, materials, type of answers or tallies desired and any variance reduction techniques used to improve the efficiency of the calculation speed). A dedicated visualization tool allows checking the geometry definition (http://www.mcnpvised.com/visualeditor/visualeditor.html).

3.5 PENELOPE

PENELOPE, an acronym for "PENetration and ENergy LOss of Positrons and Electrons" is developed by the University of Barcelona and was initially dedicated to the transport of electrons and positrons in matter. Since then, it has been completed by the addition of photon transport, for an energy range from 100 eV to 1 GeV (Salvat, 2015, Salvat and Fernández-Varea, 2009). PENELOPE is programmed in FORTRAN77 and can be started by two predefined main programs: PENCYL or PENMAIN. The main difference between these is that the geometry of PENCYL is only cylindrical while PENMAIN allows a more complete set of three-dimensional surfaces to be used. The simulation details and the geometry are described in two separate files: the input file, with the extension ".in", includes the information about the source, materials and geometry characteristics, the requested output files and the simulation conditions, and the one with the extension ".geo" contains the geometrical model. In the recent release of the code, a graphical user interface, PenGeomJar, developed under Java, facilitates geometry preparation and its two- and three-dimensional visualisation.

4. Details of results by code

4.1 General overview

The exercise was carried out by eleven participants who provided nineteen different sets of results, some participants using different versions or options of the same software or running different codes. General features of the simulation parameters are given in Table 5.

Table 5: Main simulation parameters used in the different codes

Code	Energy cuts for secondary particles	Number of channels	Detection threshold	Peak energy sigma (if applicable)	Number of generated events	Num-ber of users
EGSnrc	1 keV (e-, e+ and photons)	1000	Not applicable	Not applicable	1.0E7	1
GEANT4	0.25 keV (e-, e+ and photons)	Not applicable	1.0 keV	1.0 keV	1.0E7	4
GESPECOR	1.9 keV (photons) 10 keV (electrons)	Not applicable		Not applicable	1.0E6	2
MCNP	1 keV (e-, e+ and photons)	1000	1.0 keV	1.0 keV	1.0E8	4
PENELOPE	1 keV (e- and photons) 10 keV (e+)	1000	0.5 keV	Not applicable	1.0E7	6

Figure 3 and Figure 4 display the FEPE and TE values for detector A and B respectively, each result being obtained as the mean value of the nineteen initial data sets provided by the participants. The associated standard deviations are used to plot the uncertainty bars. As seen in Figure 3 and Figure 4, the standard deviation of each set of results is rather high, especially for the total efficiency.

Thus, a detailed analysis of the use of each code was carried out to understand the causes of the discrepancies in order to reduce them during new calculations performed in a second step. In the following, the results are presented according to the alphabetical order of the codes, with comments on the use of the software as provided by the participants.

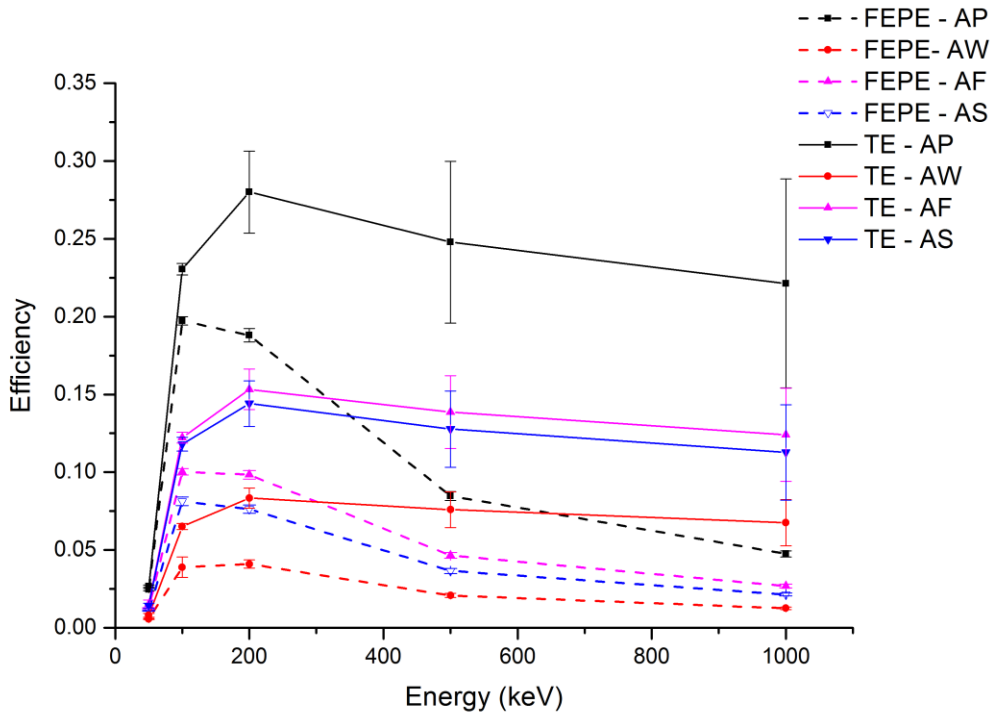

Figure 3: Mean value of the full-energy peak and total efficiencies (FEPE and TE) calculated for detector A and 4 geometries. (The plotted lines are intended only to guide the eye)

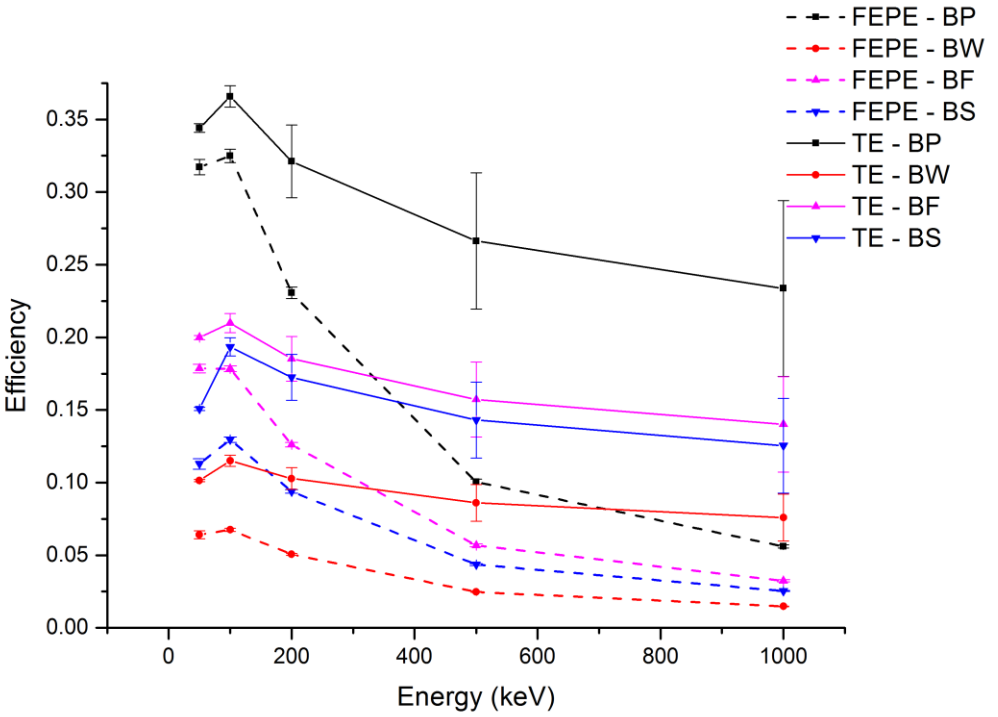

Figure 4: Mean value of the full-energy peak and total efficiencies (FEPE and TE) calculated for detector B and 4 geometries. (The plotted lines are intended only to guide the eye)

4.1 EGSnrc

One participant worked with the EGSnrc code. Table 6 presents the full-energy and total efficiencies calculated for the eight geometrical conditions, using this code.

Table 6: Calculated values and associated uncertainties obtained with EGSnrc for the eight study cases

	AP		BP		AW		BW		AF		BF		AS		BS	
E (keV)	Mean Value	Relative uncertainty (%)	Mean Value	Relative uncertainty (%)	Mean Value	Relative uncertainty (%)	Mean Value	Relative uncertainty (%)	Mean Value	Relative uncertainty (%)	Mean Value	Relative uncertainty (%)	Mean Value	Relative uncertainty (%)	Mean Value	Relative uncertainty (%)
Full-energy peak efficiency																
50	0,0243	0,20	0,3167	0,05	0,0055	0,43	0,0627	0,12	0,0126	0,28	0,1770	0,07	0,0113	0,30	0,1145	0,09
100	0,1974	0,06	0,3263	0,05	0,0404	0,15	0,0673	0,12	0,1003	0,09	0,1779	0,07	0,0811	0,11	0,1297	0,08
200	0,1893	0,07	0,2327	0,06	0,0408	0,12	0,0509	0,14	0,0989	0,10	0,1258	0,08	0,0764	0,11	0,0940	0,10
500	0,0857	0,10	0,1015	0,09	0,0210	0,17	0,0249	0,20	0,0471	0,14	0,0568	0,13	0,0370	0,16	0,0438	0,15
1000	0,0482	0,14	0,0570	0,13	0,0127	0,21	0,0151	0,26	0,0273	0,19	0,0327	0,17	0,0218	0,21	0,0257	0,19
Total efficiency																
50	0,0269	2E-05	0,3448	5E-06	0,0076	4E-05	0,1015	1E-05	0,0143	3E-05	0,2010	6E-06	0,0141	3E-05	0,1579	8E-06
100	0,2299	6E-06	0,3673	4E-06	0,0657	1E-05	0,1168	9E-06	0,1232	9E-06	0,2123	6E-06	0,1184	9E-06	0,1958	7E-06
200	0,2722	6E-06	0,3154	5E-06	0,0830	9E-06	0,1024	1E-05	0,1521	8E-06	0,1827	7E-06	0,1413	8E-06	0,1691	7E-06
500	0,2284	7E-06	0,2513	6E-06	0,0733	9E-06	0,0826	1E-05	0,1330	9E-06	0,1493	8E-06	0,1208	9E-06	0,1348	9E-06
1000	0,1941	7E-06	0,2136	7E-06	0,0636	9E-06	0,0709	1E-05	0,1158	9E-06	0,1298	9E-06	0,1034	1E-05	0,1147	9E-06

4.2 GEANT4

Four participants were using GEANT4. In a first step, small discrepancies between the individual results were noted, and it was supposed that this could be due to the difference between the electromagnetic (EM) physics used in the simulations, since there are four EM physics model available in GEANT4, quoted as:

"emstandard" standard EM physics with current 'best' options setting,
"emlivermore" low-energy EM physics using Livermore data,
"emlowenergy" low-energy EM physics implementing experimental low-energy models,
"empenelope" low-energy EM physics implementing PENELOPE models.

To clarify, complementary calculations were run with each of the four options, by the same participant (Cheick Thiam).

The results for the full-energy peak efficiencies (FEPE) and total efficiencies (TE) are presented in Figure 5 and Figure 6, respectively for detector A and detector B. For each of the five energies (E), the plotted value for each EM physics model (*i*) is the relative difference (%) compared to the mean value obtained with the four options, computed as:

$$R(E,i) = \frac{FEPE\ (E,i) - M(E)}{M(E)} \cdot 100 \qquad \text{or} \qquad R(E,i) = \frac{TE\ (E,i) - M(E)}{M(E)} \cdot 100$$

where:

$$M(E) = \frac{\sum_i FEPE(E,i)}{4} \qquad \text{or} \qquad M(E) = \frac{\sum_i TE(E,i)}{4}$$

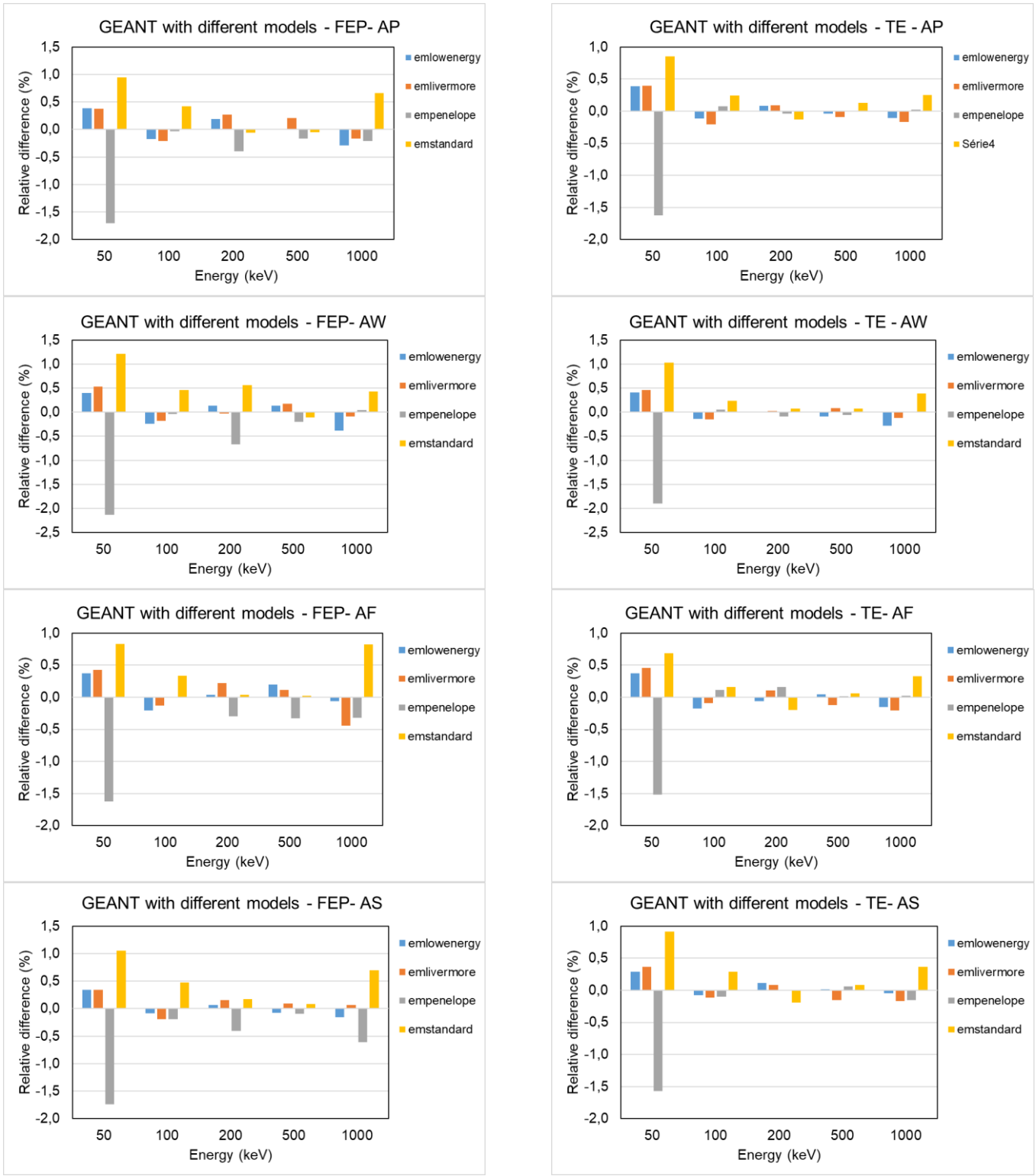

Figure 5: For each GEANT4 option, difference relative to the mean value for detector A and the four study cases (left side: full-energy peak efficiency; right side: total efficiency)

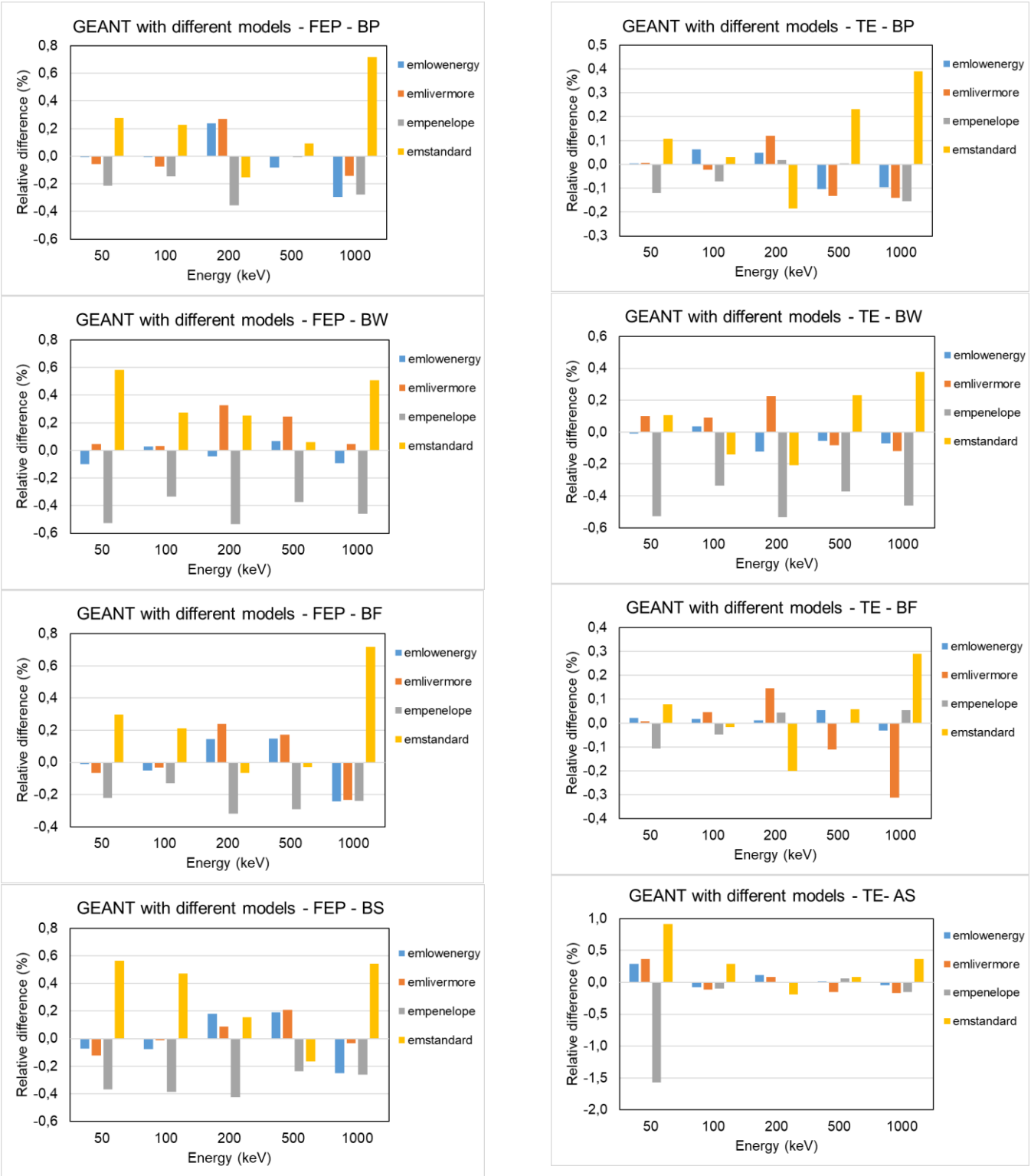

Figure 6: For each GEANT4 option, difference relative to the mean value for detector B and the four study cases (left side: full-energy peak efficiency; right side: total efficiency)

The presented results clearly demonstrate that the “emstandard” and “empenelope” models provide slightly different results than those obtained with the two other options, mainly for the 50-keV cases.
A summary of these results is presented in
Figure 7 and Figure 8, respectively for detector A and detector B, where “*Di*” is plotted as the quadratic sum of the relative differences, computed as:

$$Di = \sum_E \left(\frac{FEPE\,(E,i) - M(E)}{M(E)} \cdot 100\right)^2 \qquad \text{(E = 50 keV, 100 keV, 200 keV, 500 keV, 1000 keV)}$$

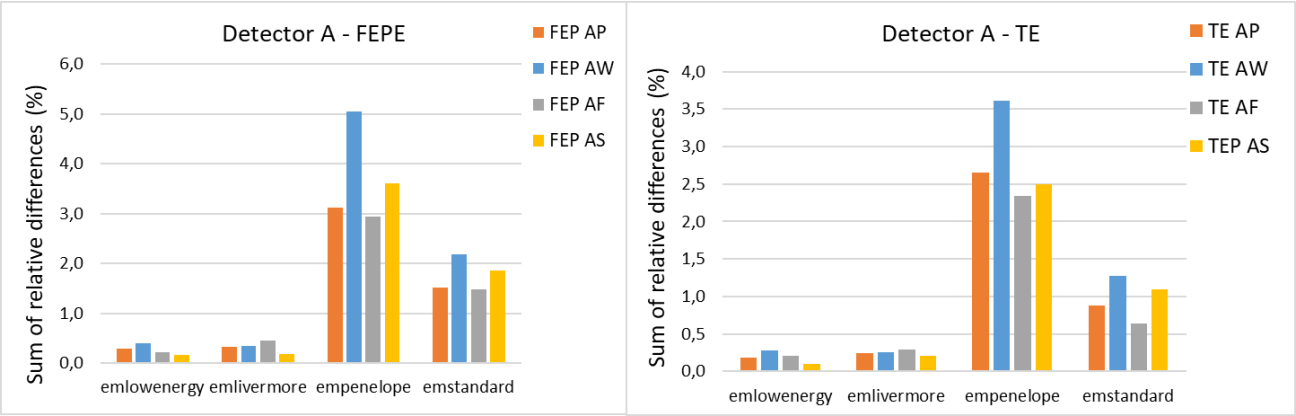

Figure 7: Summary of GEANT4 tests for detector A and the four study cases using 4 options: quadratic sum (of the 5 energies) of the relative differences (%) related to the mean value.

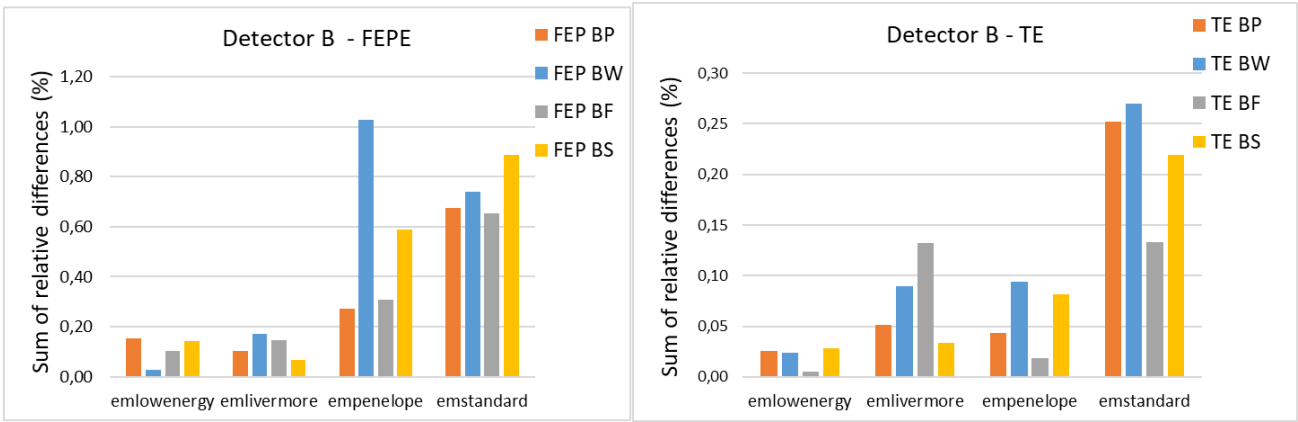

Figure 8: Summary of GEANT4 test for detector B and the four study cases using 4 options: quadratic sum (of the 5 energies) of the relative differences (%) related to the mean value

To summarize and for comparison with the other codes, Table 7 presents the mean value of the results obtained by the GEANT4 users, and the relative standard deviation between the results. These show a rather good homogeneity with relative standard deviations lower than 1 % for most of the cases.

It must be mentioned that these results are those obtained with the “empenelope” option, as agreed by the participants, to give the opportunity to provide a more direct comparison with the results of PENELOPE users.

Table 7: Mean values and standard deviations of the GEANT4 participants’ results for the eight study cases

	AP		BP		AW		BW		AF		BF		AS		BS	
E (keV)	Mean value	Standard deviation (%)	Mean value	Standard deviation (%)	Mean value	Standard deviation (%)	Mean value	Standard deviation (%)	Mean value	Standard deviation (%)	Mean value	Standard deviation (%)	Mean value	Standard deviation (%)	Mean value	Standard deviation (%)
Full-energy peak efficiency																
50	0,0248	1,08	0,3199	0,14	0,0059	1,06	0,0656	2,33	0,0129	1,29	0,1802	0,12	0,0114	0,81	0,1152	0,20
100	0,1982	0,17	0,3271	0,18	0,0411	0,18	0,0682	0,40	0,1012	0,28	0,1794	0,13	0,0818	0,03	0,1306	0,22
200	0,1896	0,25	0,2328	0,28	0,0409	0,38	0,0508	0,50	0,0995	0,18	0,1268	0,22	0,0770	0,35	0,0946	0,35
500	0,0854	0,45	0,1015	0,07	0,0209	0,34	0,0250	0,38	0,0472	0,28	0,0569	0,20	0,0368	0,76	0,0437	0,34
1000	0,0479	0,27	0,0565	0,28	0,0127	1,12	0,0150	0,53	0,0272	0,32	0,0326	0,58	0,0216	0,36	0,0255	0,63
Total efficiency																
50	0,0269	1,16	0,3448	0,14	0,0076	1,09	0,1014	0,13	0,0143	1,34	0,1999	0,07	0,0136	0,87	0,1504	0,17
100	0,2276	0,13	0,3628	0,13	0,0636	0,29	0,1121	0,22	0,1202	0,18	0,2061	0,18	0,1156	0,15	0,1895	0,29
200	0,2708	0,12	0,3127	0,13	0,0814	0,11	0,0993	0,11	0,1499	0,14	0,1794	0,22	0,1398	0,21	0,1660	0,22
500	0,2270	0,21	0,2502	0,12	0,0725	0,15	0,0814	0,15	0,1319	0,12	0,1480	0,12	0,1199	0,19	0,1333	0,25
1000	0,1930	0,10	0,2125	0,19	0,0629	0,14	0,0697	0,18	0,1146	0,23	0,1284	0,25	0,1024	0,17	0,1137	0,32

The deviation of individual results relative to the mean value (%) are presented in Figure 9 and Figure 10, for the full-energy peak efficiency and total efficiency, respectively.

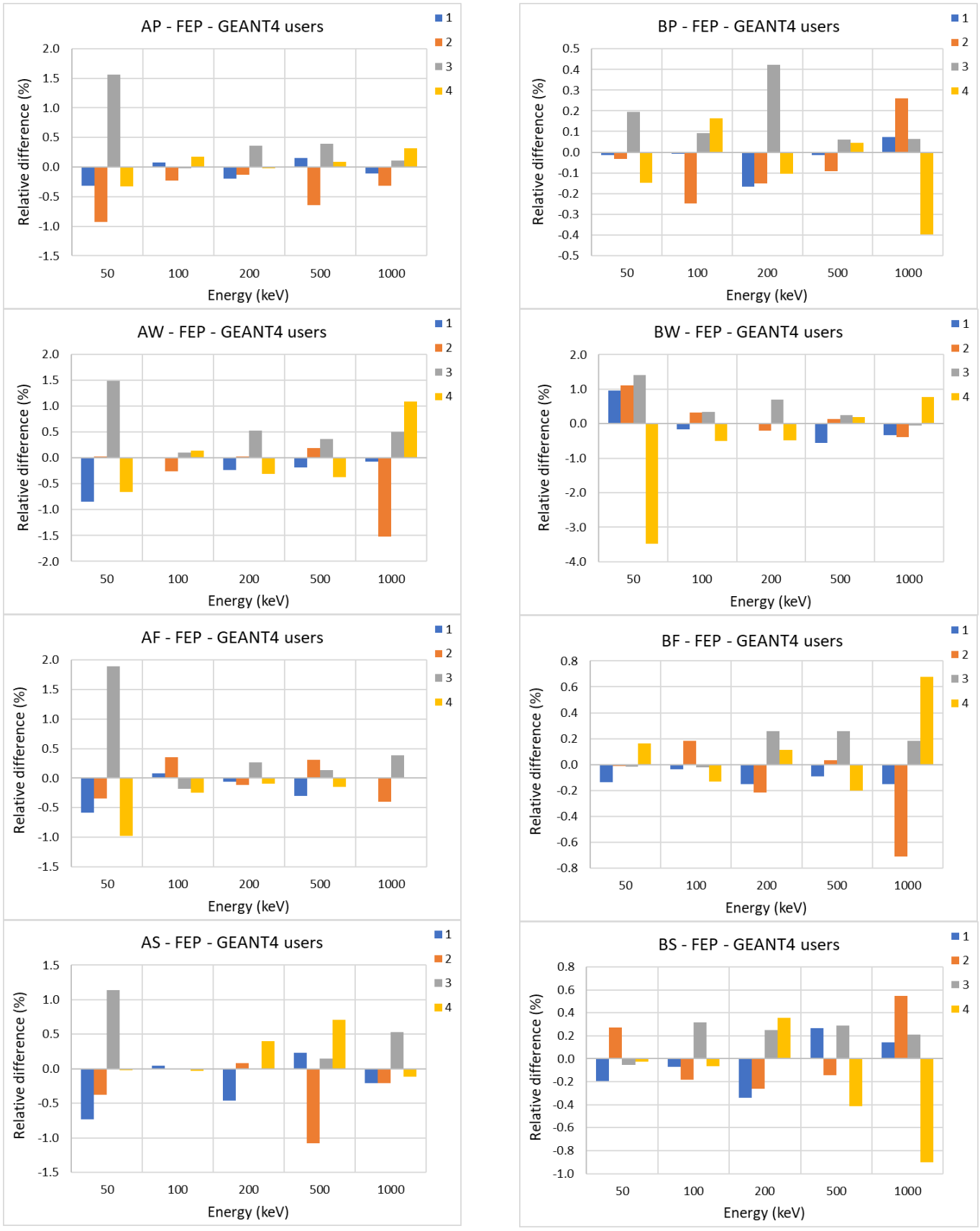

Figure 9: Differences relative to the mean values (%) of GEANT4 users (numbers 1 to 4) for the full-energy peak efficiency

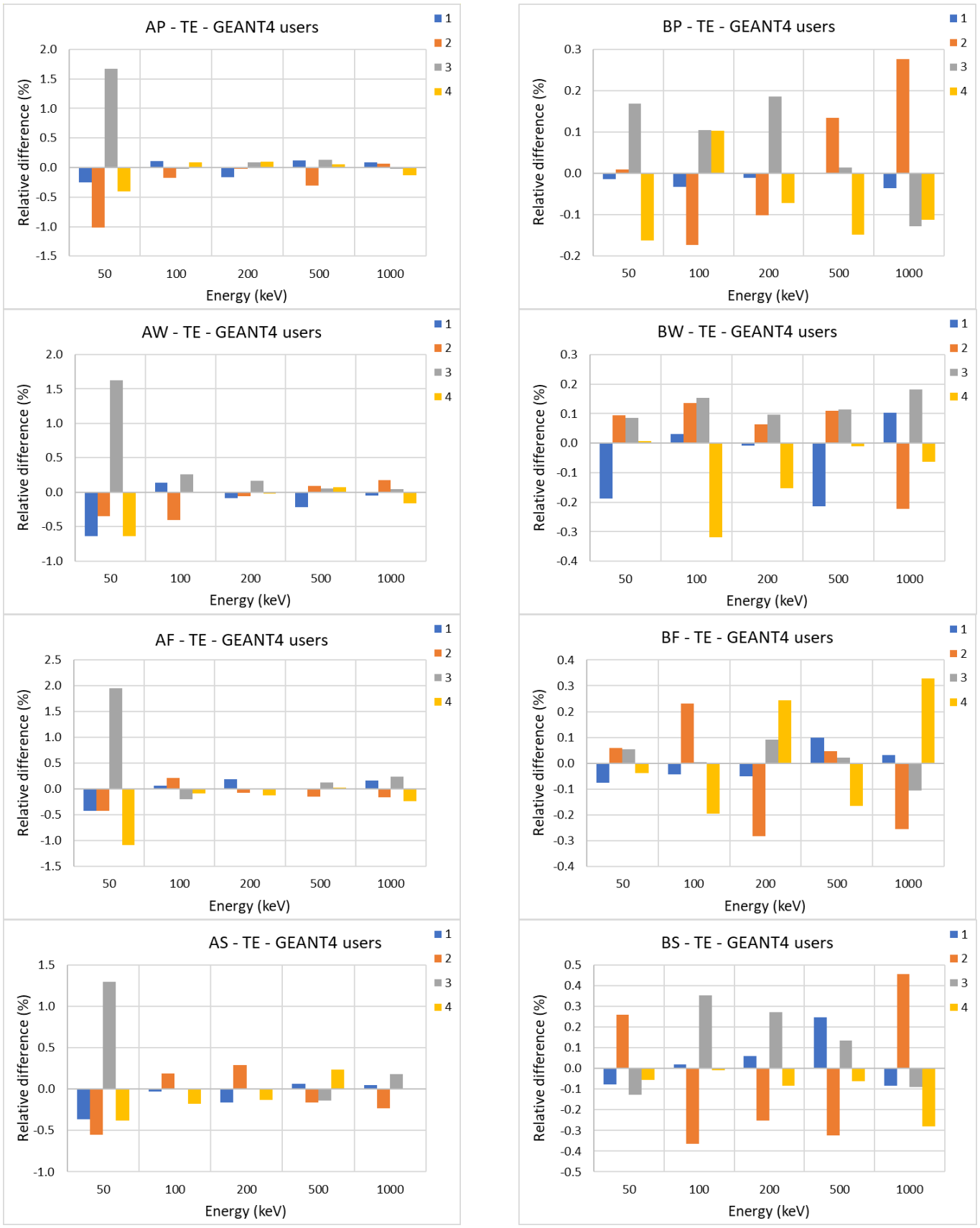

Figure 10: Differences relative to the mean values (%) of GEANT 4 users (numbers 1 to 4) for the total efficiency

4.3 GESPECOR

GESPECOR version 4.2 was used by two participants. The summary of the results are presented in Table 8.

Table 8: Mean values and standard deviations of the GESPECOR participants' results for the eight study cases

	AP		BP		AW		BW		AF		BF		AS		BS	
E (keV)	Mean Value	Relative standard deviation (%)	Mean Value	Relative standard deviation (%)	Mean Value	Relative standard deviation (%)	Mean Value	Relative standard deviation (%)	Mean Value	Relative standard deviation (%)	Mean Value	Relative standard deviation (%)	Mean Value	Relative standard deviation (%)	Mean Value	Relative standard deviation (%)
Full-energy peak efficiency																
50	0.0238	0.02	0.3058	0.01	0.0053	0.01	0.0608	0.11	0.0120	0.10	0.1719	0.02	0.0102	0.28	0.1070	0.11
100	0.1899	0.02	0.3158	0.00	0.0378	0.08	0.0653	0.00	0.0946	0.00	0.1732	0.02	0.0747	0.02	0.1251	0.04
200	0.1765	0.00	0.2237	0.06	0.0372	0.04	0.0490	0.18	0.0909	0.11	0.1220	0.05	0.0694	0.39	0.0906	0.14
500	0.0771	0.13	0.0971	0.13	0.0184	0.22	0.0238	0.07	0.0416	0.08	0.0546	0.14	0.0324	0.31	0.0418	0.18
1000	0.0426	0.12	0.0541	0.01	0.0110	0.17	0.0143	0.35	0.0236	0.21	0.0311	0.09	0.0189	0.25	0.0244	0.27
Total efficiency																
50	0.0429	0.34	0.3394	0.17	0.0111	0.68	0.0994	0.17	0.0224	0.21	0.1966	0.17	0.0185	0.45	0.1485	0.20
100	0.2291	0.15	0.3543	0.11	0.0627	0.54	0.1098	0.00	0.1184	0.03	0.2011	0.26	0.1121	0.27	0.1865	0.09
200	0.2533	0.04	0.3032	0.13	0.0753	0.08	0.0971	0.03	0.1376	0.23	0.1742	0.01	0.1282	0.56	0.1625	0.26
500	0.2085	0.00	0.2432	0.04	0.0656	0.65	0.0793	0.45	0.1187	0.11	0.1440	0.27	0.1086	0.28	0.1311	0.34
1000	0.1765	0.01	0.2046	0.09	0.0567	0.64	0.0681	0.51	0.1026	0.39	0.1237	0.09	0.0922	0.32	0.1103	0.43

Excellent agreement is observed between both series of calculations, since the resulting standard deviations between them is low. The deviation of individual results relative to the mean value (%) are presented in Figure 11 and Figure 12, for the full-energy peak efficiency and total efficiency, respectively. As expected, since there are only two outcomes, the relative differences are simply opposite numbers.

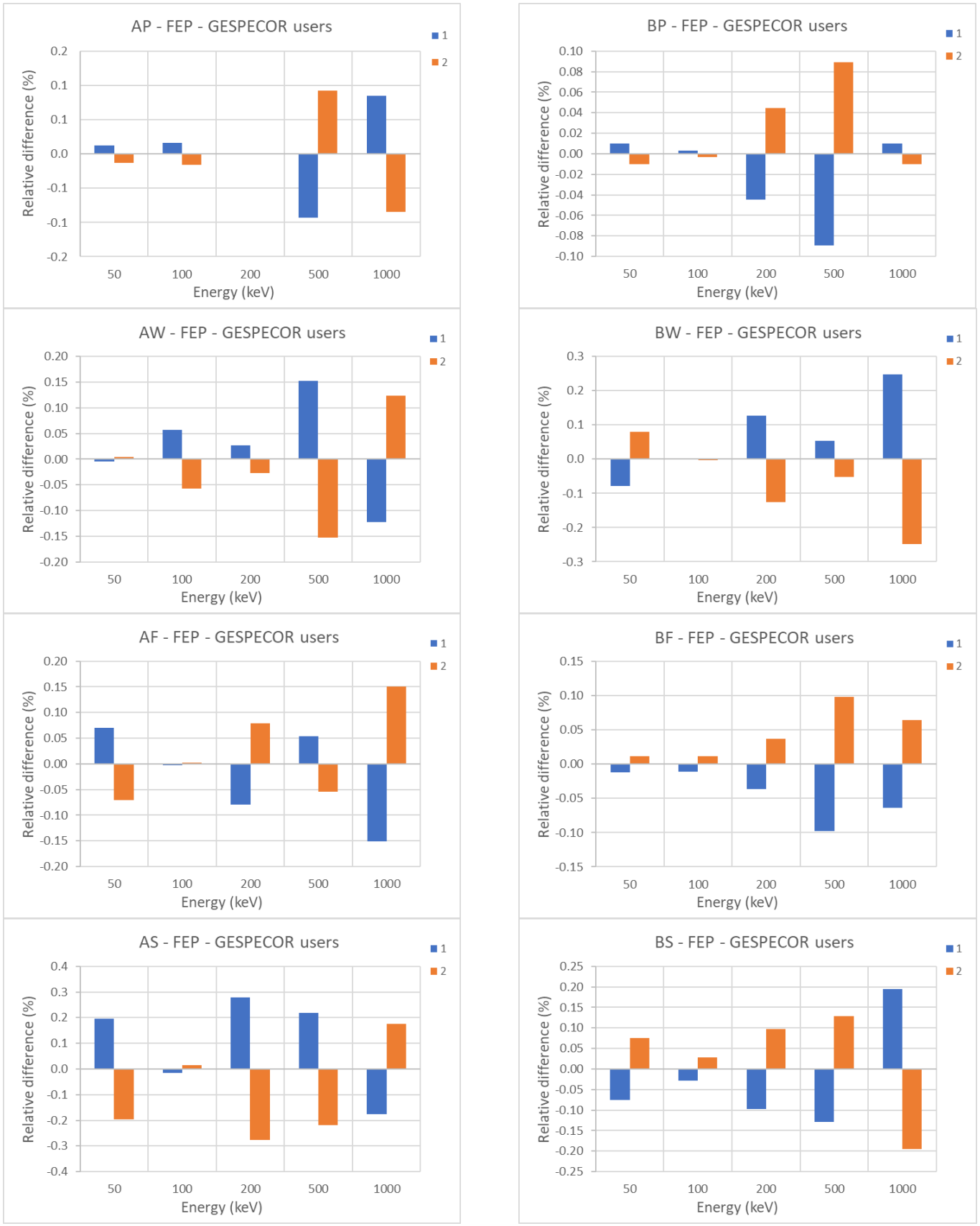

Figure 11: Differences relative to the mean values (%) of GESPECOR users (numbers 1 and 2) for the full-energy peak efficiency

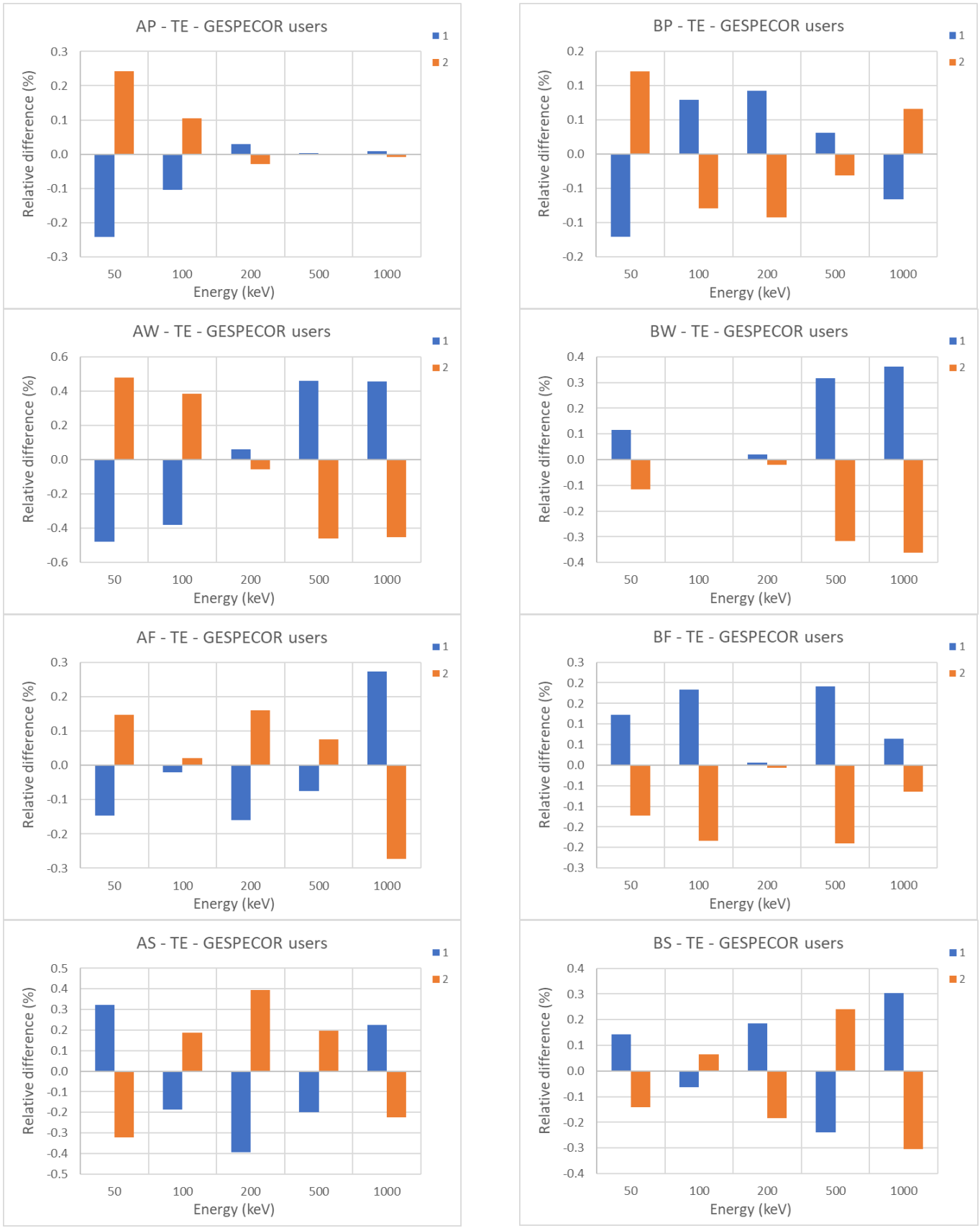

Figure 12: Differences relative to the mean values (%) of GESPECOR users (numbers 1 and 2) for the total efficiency

4.4 MCNP

4.4.1 General results

Four participants were using MCNP in this exercise. Table 9 presents the mean value of the results obtained by MCNP users and the relative standard deviations between these. The calculations for the FEP efficiencies show a rather good homogeneity of results with relative standard deviations lower than 1 % for most of the cases; some higher discrepancies may be due to the weak efficiencies (low energy) and lack of statistics. Conversely, large deviations affect the TE results, especially for high energies, with relative differences of up to 30 %.

Table 9: Mean values and standard deviations of the MCNP participants' results for the eight study cases

	AP		BP		AW		BW		AF		BF		AS		BS	
E (keV)	Mean value	Standard deviation (%)	Mean value	Standard deviation (%)	Mean value	Standard deviation (%)	Mean value	Standard deviation (%)	Mean value	Standard deviation (%)	Mean value	Standard deviation (%)	Mean value	Standard deviation (%)	Mean value	Standard deviation (%)
Full-energy peak efficiency																
50	0.0241	3.08	0.3176	1.54	0.0056	3.31	0.0641	2.66	0.0125	2.80	0.1798	0.62	0.0113	2.28	0.1126	1.85
100	0.1979	0.32	0.3244	1.91	0.0407	0.86	0.0675	0.69	0.1008	0.38	0.1793	0.26	0.0833	0.68	0.1298	0.54
200	0.1898	0.68	0.2302	2.38	0.0408	0.33	0.0508	0.13	0.0994	0.42	0.1268	0.65	0.0783	0.14	0.0942	0.14
500	0.0864	2.03	0.1003	2.66	0.0209	0.04	0.0249	0.11	0.0474	1.67	0.0574	1.73	0.0377	0.14	0.0438	0.11
1000	0.0485	3.07	0.0560	2.84	0.0127	0.23	0.0149	0.13	0.0275	2.45	0.0329	2.59	0.0221	0.13	0.0256	0.22
Total efficiency																
50	0.0263	3.53	0.3438	1.34	0.0076	0.93	0.1019	0.61	0.0139	4.01	0.2011	0.67	0.0138	0.75	0.1514	0.74
100	0.2337	2.45	0.3724	2.39	0.0672	3.72	0.1190	4.05	0.1260	4.07	0.2180	3.99	0.1243	3.99	0.2014	4.39
200	0.3091	11.0	0.3534	10.4	0.0920	9.9	0.1132	10.3	0.1712	10.9	0.2068	11.3	0.1650	12.3	0.1944	12.8
500	0.3052	22.8	0.3289	22.0	0.0918	19.0	0.1036	19.3	0.1715	20.5	0.1937	20.9	0.1627	22.7	0.1795	23.2
1000	0.2947	31.0	0.3148	30.1	0.0882	26.0	0.0983	26.1	0.1664	27.7	0.1865	27.8	0.1561	30.1	0.1709	30.4

The deviations of individual results relative to the mean value (%) are presented in Figure 13 for the full-energy peak efficiency. It can be noted that some discrepant results significantly affect the mean value and, consequently, the relative differences. However, this is not systematic, except for a series of results (1) calculated for a geometry without shielding, which was withdrawn from the results presented in Table 9, Figure 13 and Figure 14. Specific analysis of the shielding is detailed in section 4.4.2.
Figure 14 shows the deviation of individual results relative to the mean value (%) for the total efficiency. Actually, the large relative deviations quoted in Figure 14 reveal discrepancies between two groups of results (2 and 5) and (3, 4 and 6).

Note: it should be noted (MCNP manual) that "The zero bin will catch non analog knock-on electron negative scores. The epsilon (1E–5) bin will catch scores from particles that travel through the cell without depositing energy. See Chapter 2 page 2–89", thus, small differences on the total efficiency may be due to a misuse of these energy bins.

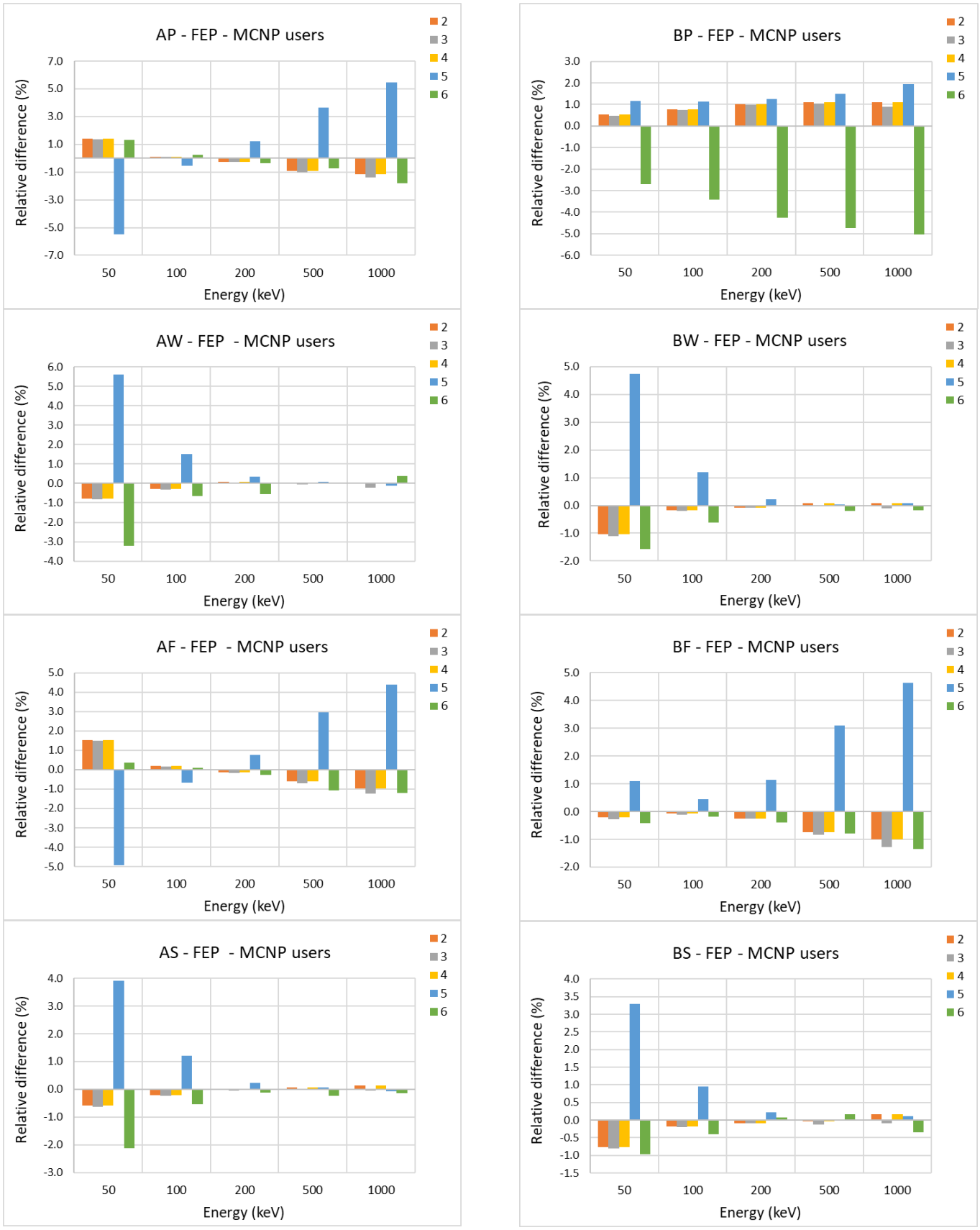

Figure 13: Differences relative to the mean values (%) of MCNP users (numbers 2 to 6) for the full-energy peak efficiency

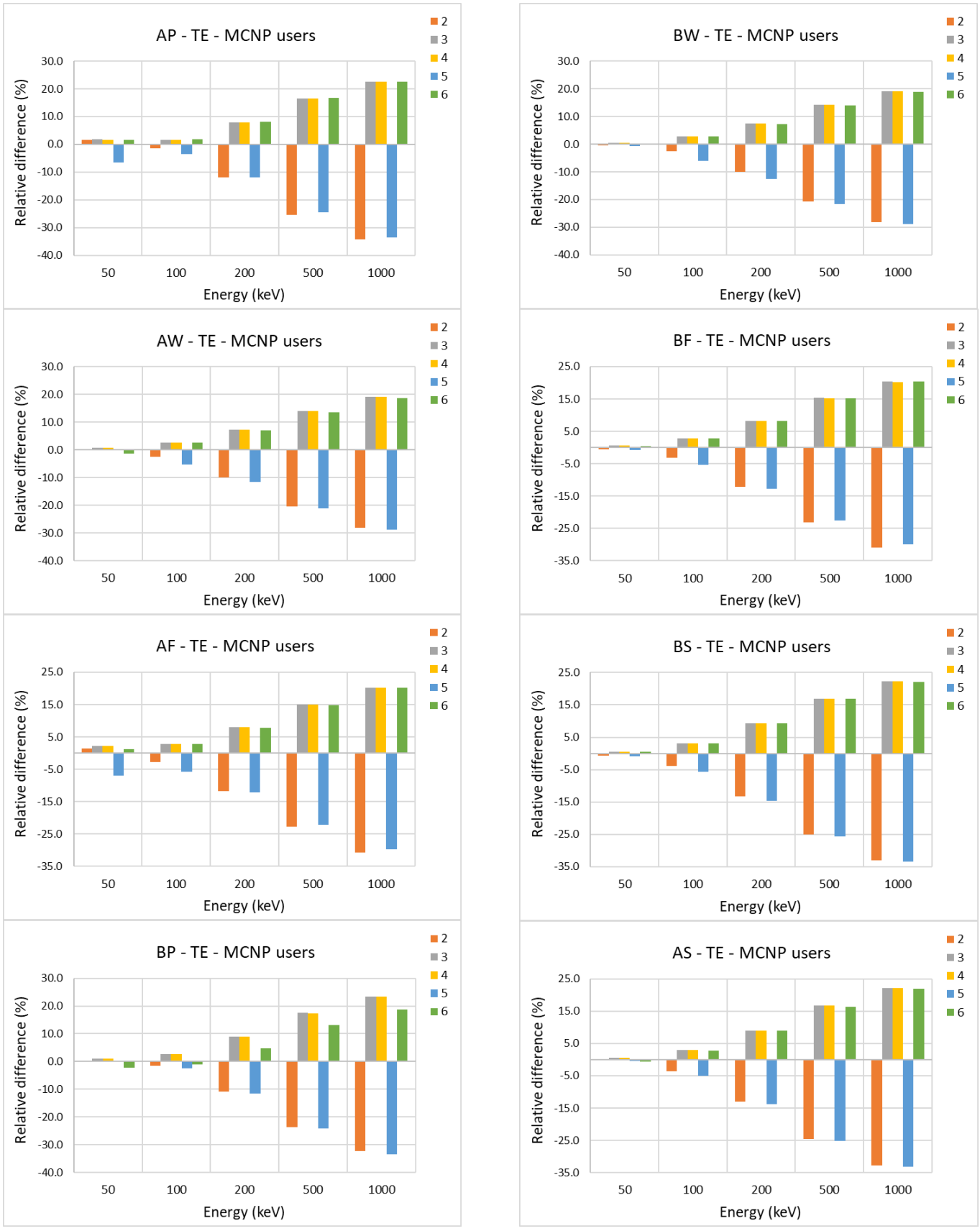

Figure 14: Differences relative to the mean values of MCNP users (numbers 2 to 6) for the total efficiency

4.4.2 Complementary analyses

Most of the participants used version 6 of MCNP. However, Theodora Vasilopoulou performed the same computation using versions 5 and 6 and did not notice any difference.
Cheick Thiam studied the effect on the binning by changing the maximum energy taken into consideration (*i.e.*, more bins for the low energies). This has a negligible effect on the total efficiencies, but, as expected, there are noticeable differences for FEP efficiencies at 50 keV while there is no change at 1 MeV, as displayed in Figure 15.

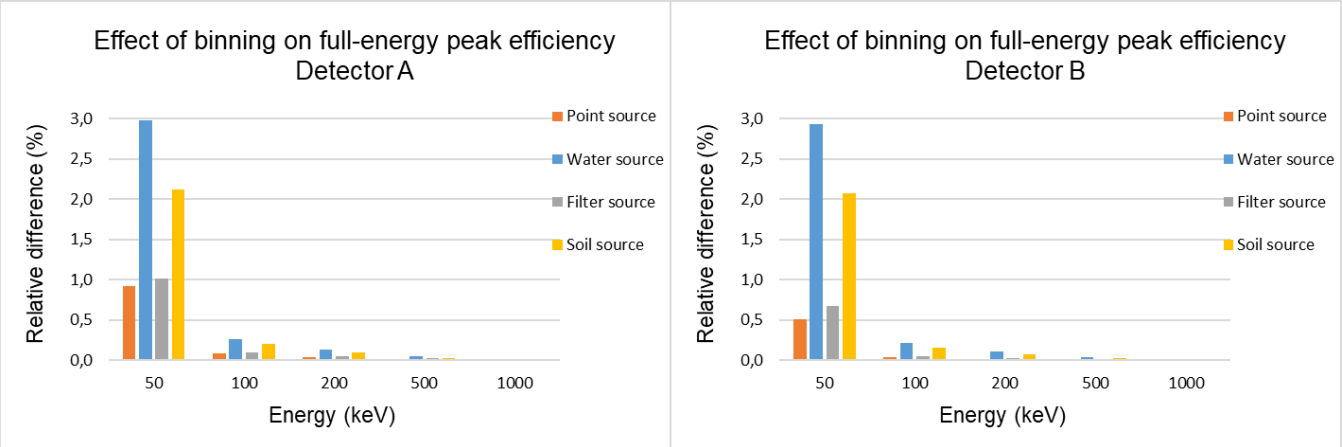

Figure 15: Relative difference (%) due to the change of binning

Cheick Thiam also examined the effect of the energy width of the simulated peaks (parameter = "peak energy sigma"), changing it to 2 keV instead of 1 keV. Differences of a few percent for the FEP and volume sources at low energies are visible: this may be due to the scattering effect which is more important in the low energy range, inducing events close to the full-energy peak that are included in it, which, consequently increase the peak area.

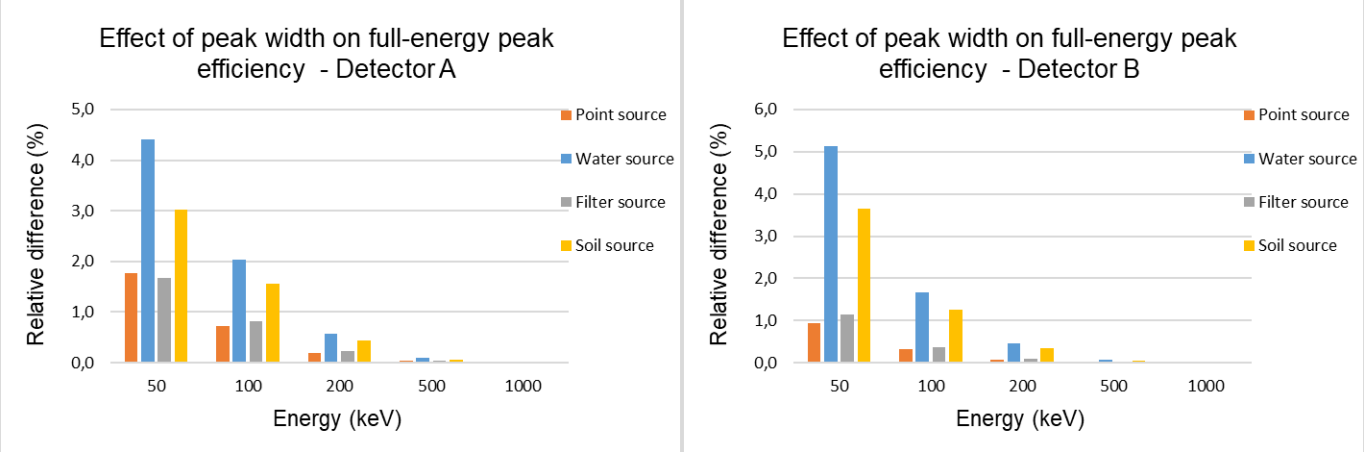

Figure 16: Relative difference (%) due to the change of peak width

Complementary calculations were also performed by Tran Thien Thanh to demonstrate the influence of the shielding on the efficiency computation results. While there was no significant difference for the FEP efficiencies, it was seen that the total efficiency was underestimated by about 2%-3% when the shielding is not included, as shown in Figure 17.

Figure 17: Relative difference (%) due to the presence of shielding

Of course, the shielding has also a direct influence on the spectral shape through scattering effects and the presence of X-ray lines from lead fluorescence, particularly for E =100 keV. Figure *18* and Figure *19* show the simulated spectra for the case of 100 keV photons from a filter, for detector A and detector B, respectively. In this case, the relative differences on the total efficiency (with shielding/without shielding) are 1.69 % for detector A and 2.19 % for detector B.

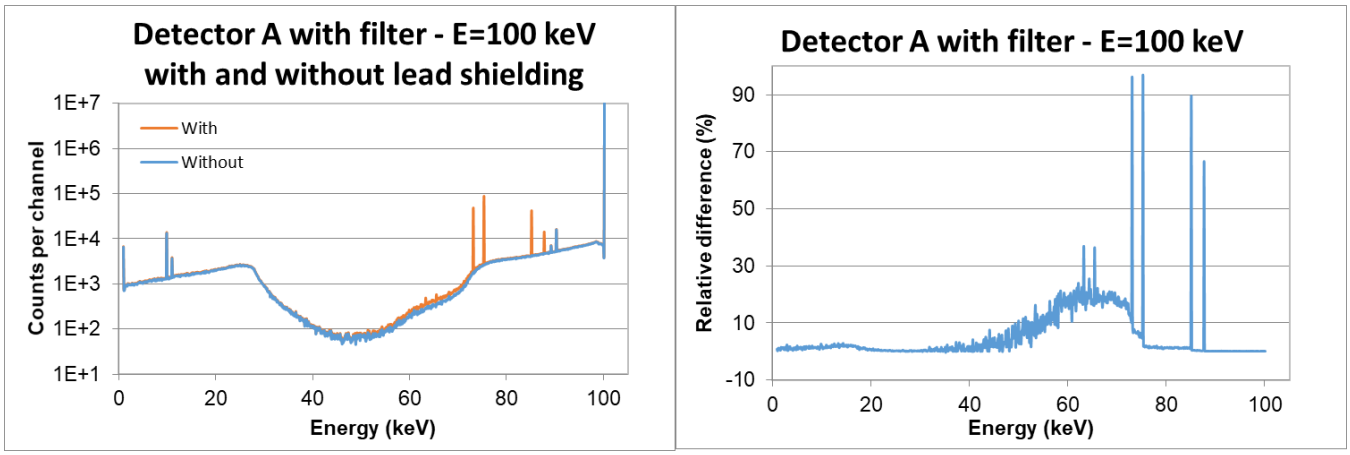

Figure 18: Monte Carlo simulation of detector A with filter and 100-keV photons, with and without lead shielding. Left panel: superimposed simulations – Right panel: relative differences (%)

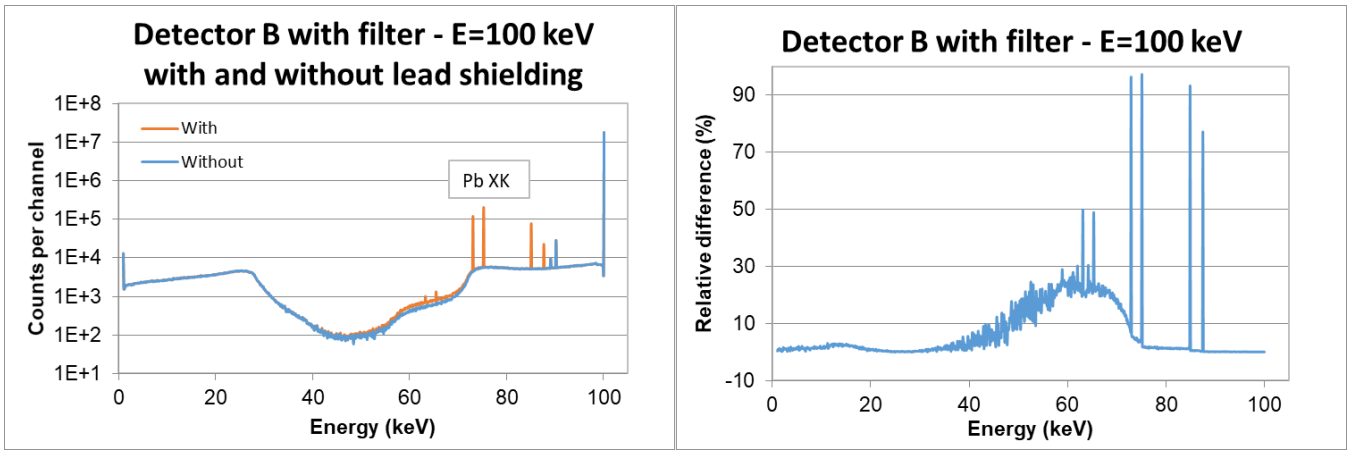

Figure 19: Monte Carlo simulation of detector B with filter and 100-keV photons, with and without lead shielding. Left panel: superimposed simulations – Right panel: relative differences (%)

The summary of the relative differences between simulations of the total efficiency performed without and with shielding for all study cases is presented in Table 10.

Table 10: Relative difference (%) of the total efficiency computed without and with shielding

Energy	AP	BP	AW	BW	AF	BF	AS	BS
50	-0.02	-0.03	-0.15	-0.11	-0.08	-0.06	-0.05	-0.05
100	-0.68	-1.00	-2.70	-3.43	-1.69	-2.19	-1.39	-1.94
200	-0.32	-0.59	-1.49	-2.55	-0.71	-1.22	-0.77	-1.39
500	-0.18	-0.26	-0.80	-1.19	-0.36	-0.51	-0.43	-0.64
1000	-0.19	1.23	-0.77	-0.99	-0.36	-0.43	-0.42	-0.55

4.5 PENELOPE

Six participants provided results with PENELOPE, using versions 2014, or 2016. The mean value of the results obtained by the PENELOPE users, and the relative standard deviation between the results are presented in Table 11. These show a good consistency with relative standard deviations lower than 1% for all cases.

Table 11: Mean values and standard deviations of the PENELOPE participants' results for the eight study cases

	AP		BP		AW		BW		AF		BF		AS		BS	
E (keV)	Mean value	Standard deviation (%)	Mean value	Standard deviation (%)	Mean value	Standard deviation (%)	Mean value	Standard deviation (%)	Mean value	Standard deviation (%)	Mean value	Standard deviation (%)	Mean value	Standard deviation (%)	Mean value	Standard deviation (%)
Full-energy peak efficiency																
50	0.0244	0.87	0.3171	0.18	0.0056	0.85	0.0629	0.35	0.0127	0.40	0.1778	0.11	0.0110	0.72	0.1113	0.41
100	0.1979	0.13	0.3262	0.13	0.0406	0.30	0.0673	0.30	0.1009	0.24	0.1786	0.16	0.0810	0.19	0.1293	0.19
200	0.1887	0.36	0.2315	0.22	0.0407	0.37	0.0506	0.53	0.0991	0.05	0.1261	0.09	0.0763	0.34	0.0939	0.13
500	0.0849	0.72	0.1008	0.19	0.0208	0.56	0.0247	0.38	0.0469	0.33	0.0567	0.44	0.0367	0.21	0.0437	0.38
1000	0.0478	0.28	0.0563	0.14	0.0126	0.44	0.0149	0.65	0.0271	0.44	0.0323	0.30	0.0215	0.76	0.0254	0.44
Total efficiency																
50	0.0270	0.86	0.3451	0.21	0.0077	0.63	0.1015	0.37	0.0143	0.40	0.1999	0.06	0.0137	0.53	0.1509	0.17
100	0.2302	0.10	0.3665	0.19	0.0657	0.35	0.1164	0.32	0.1229	0.13	0.2107	0.26	0.1178	0.11	0.1941	0.17
200	0.2709	0.59	0.3138	0.46	0.0826	0.47	0.1015	0.70	0.1509	0.29	0.1813	0.48	0.1406	0.43	0.1684	0.44
500	0.2270	0.53	0.2502	0.28	0.0730	0.51	0.0822	0.30	0.1321	0.59	0.1484	0.50	0.1203	0.42	0.1343	0.36
1000	0.1939	0.28	0.2128	0.27	0.0633	0.19	0.0706	0.25	0.1151	0.12	0.1288	0.17	0.1031	0.14	0.1142	0.12

The deviations of individual results relative to the mean value (%) are presented in Figure *20* and *Figure 21*, for the full-energy peak efficiencies and the total efficiencies, respectively.

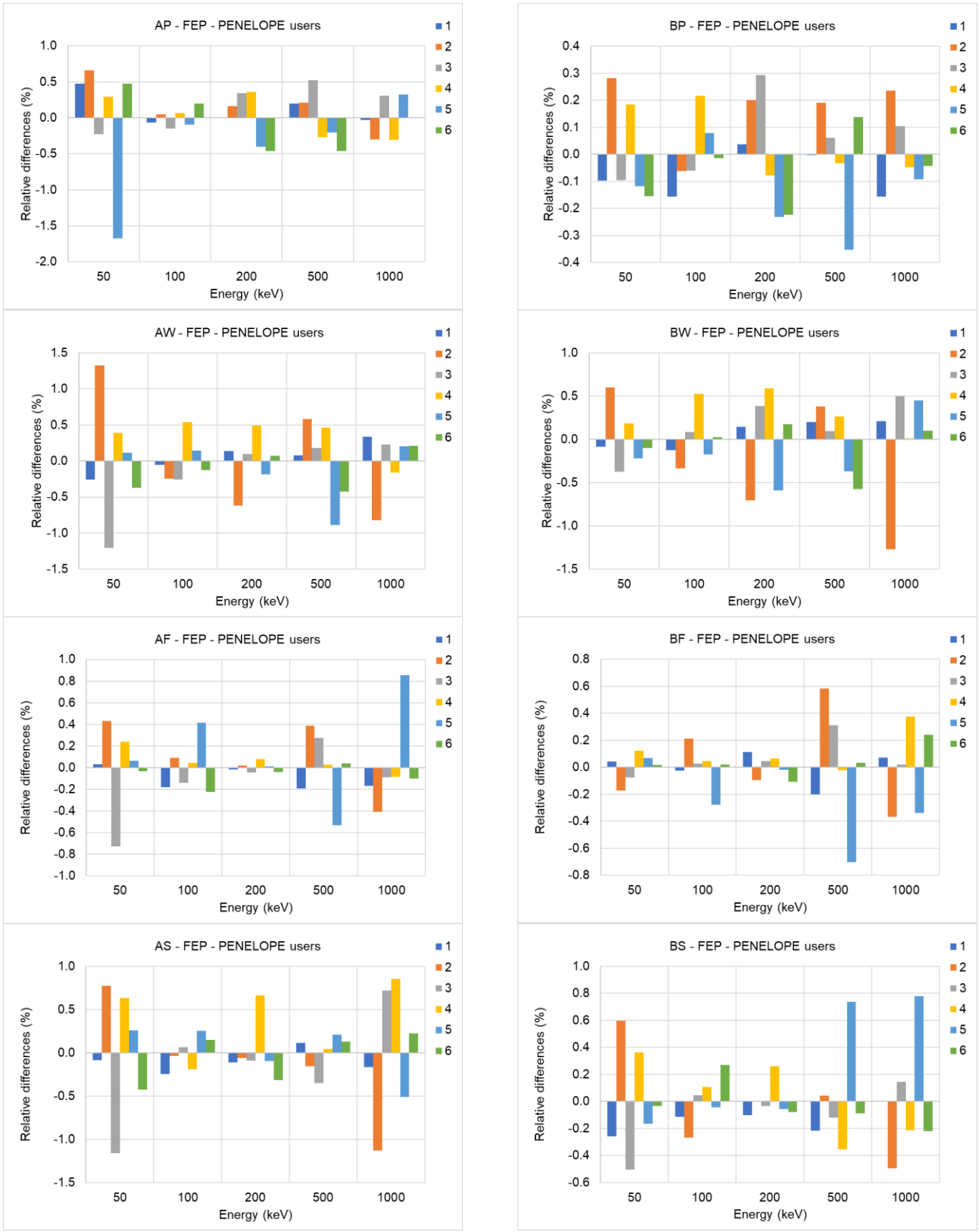

Figure 20: Differences relative to the mean values (%) of PENELOPE users (numbers 1 to 6) for the full-energy peak efficiency

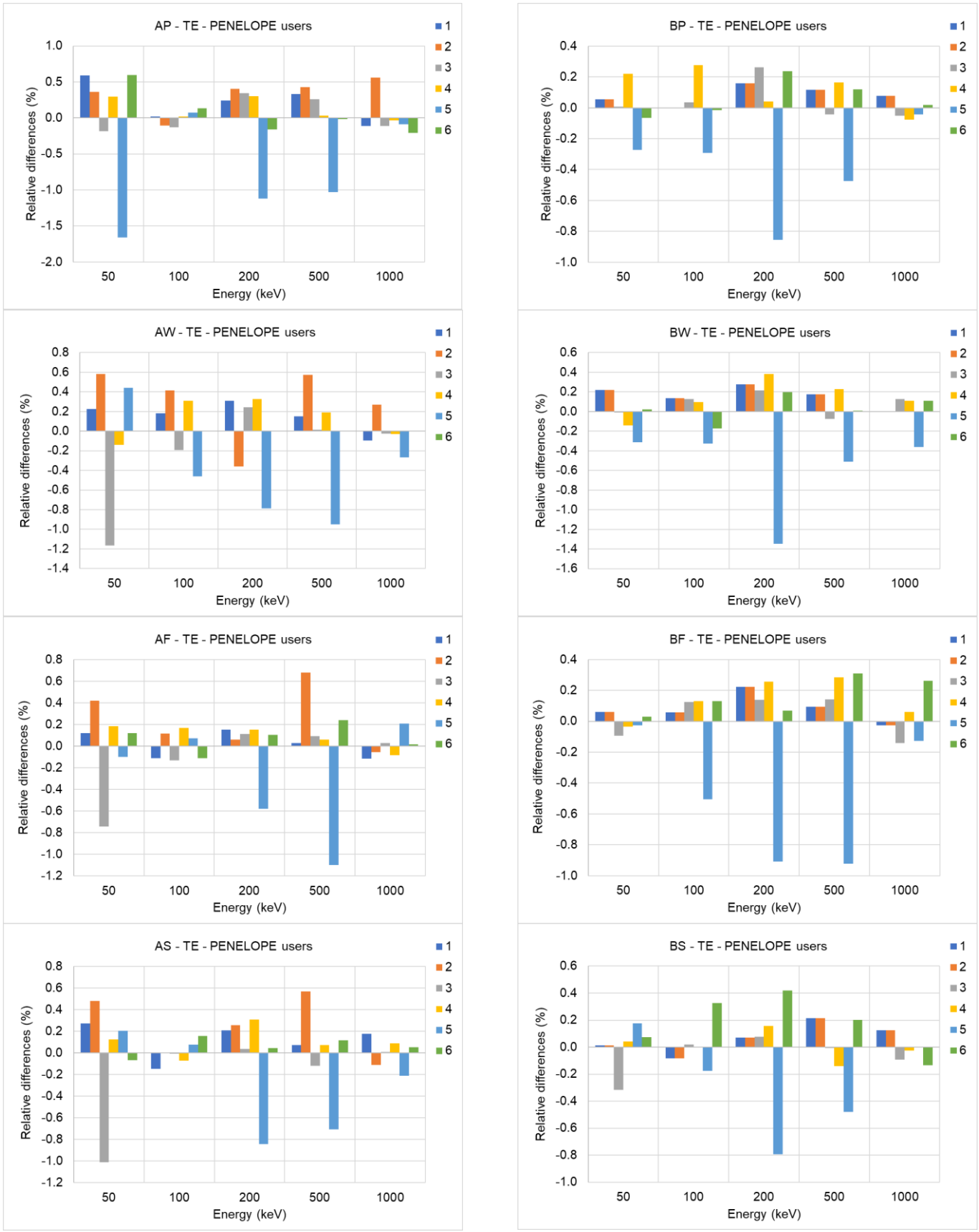

Figure 21: Differences relative to the mean values (%) of PENELOPE users (numbers 1 to 6) for the total efficiency

5. General results

For the final compilation of results, all data were carefully checked, eventually revised, and a few of these were rejected in view of evident discrepancies. Figure 22 and Figure 23 display the FEP and total efficiency values for detector A and B respectively, each point representing the mean value of the final data sets provided by participants. These can be compared to the initial values (Figure 3 and Figure 4); here, it can be noted that the standard deviations used to plot the associated uncertainty bars are barely visible, showing that the final set of data is rather consistent.

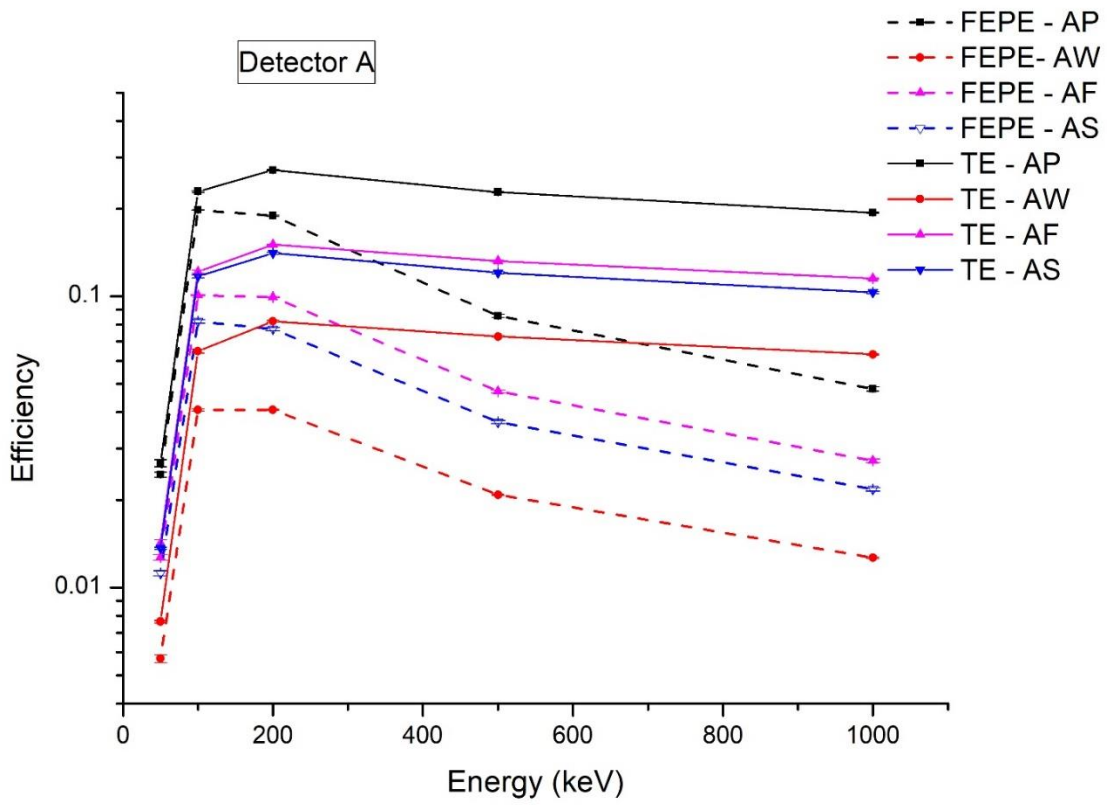

Figure 22: Final mean value of the full-energy peak and total efficiencies (FEPE and TE) calculated for detector A for the four study cases. (The plotted lines are intended only to guide the eye)

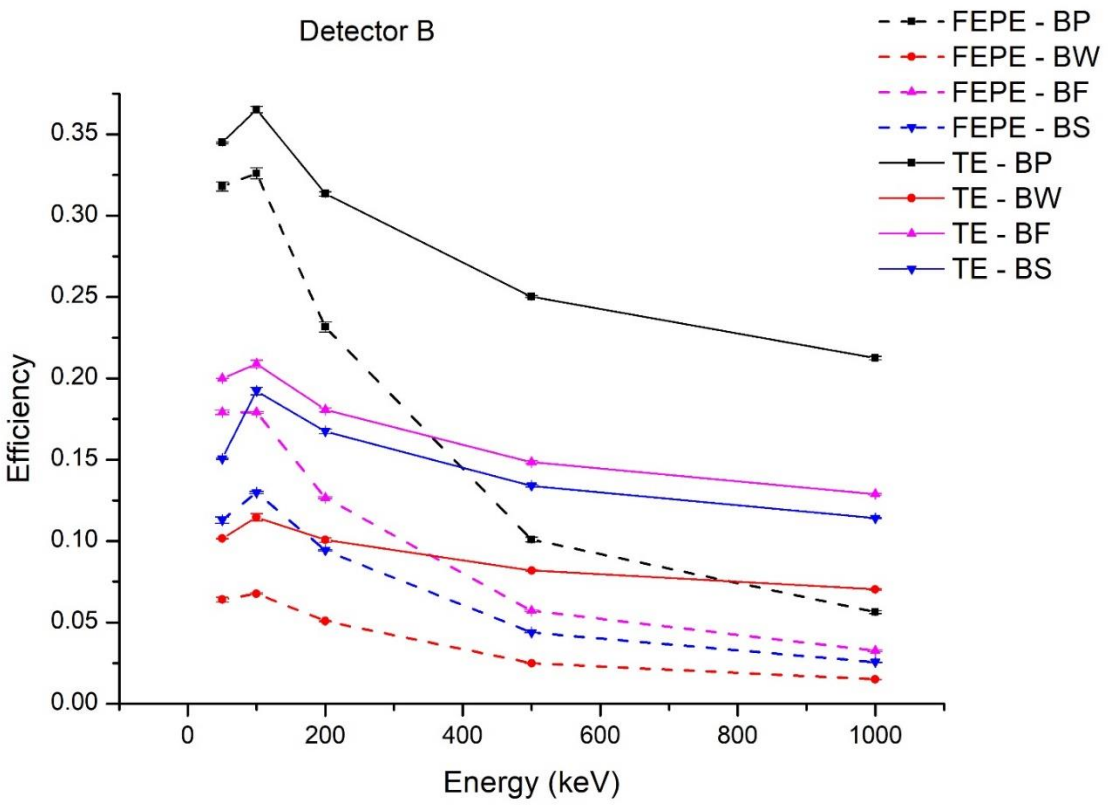

Figure 23: Final mean value of the full-energy peak and total efficiencies (FEPE and TE) calculated for detector B for the four study cases. (The plotted lines are intended only to guide the eye)

The final results are summarized in Table 12, which shows the mean values obtained after checking of the results and rejection of a few discrepant data.

Table 12: Mean values and standard deviations of the participants' final results for the eight study cases

	AP		BP		AW		BW		AF		BF		AS		BS	
E (keV)	Mean Value	Relative standard deviation (%)	Mean Value	Relative standard deviation (%)	Mean Value	Relative standard deviation (%)	Mean Value	Relative standard deviation (%)	Mean Value	Relative standard deviation (%)	Mean Value	Relative standard deviation (%)	Mean Value	Relative standard deviation (%)	Mean Value	Relative standard deviation (%)
Full-energy peak efficiency																
50	0.0244	2.10	0.3180	0.91	0.0057	3.01	0.0640	2.50	0.0127	2.10	0.1791	0.71	0.0112	2.06	0.1128	1.76
100	0.1980	0.21	0.3258	1.08	0.0408	0.76	0.0676	0.73	0.1009	0.32	0.1791	0.28	0.0820	1.29	0.1298	0.51
200	0.1893	0.52	0.2314	1.36	0.0408	0.44	0.0507	0.49	0.0993	0.31	0.1265	0.46	0.0772	1.18	0.0942	0.36
500	0.0856	1.32	0.1008	1.49	0.0208	0.43	0.0248	0.52	0.0471	1.02	0.0570	1.13	0.0370	1.31	0.0437	0.33
1000	0.0481	1.80	0.0562	1.57	0.0126	0.64	0.0149	0.54	0.0273	1.49	0.0326	1.66	0.0218	1.29	0.0255	0.50
Total efficiency																
50	0.0267	2.71	0.3449	0.17	0.0076	1.00	0.1015	0.28	0.0142	2.90	0.1998	0.07	0.0136	0.80	0.1506	0.24
100	0.2289	0.75	0.3650	0.55	0.0648	1.69	0.1145	1.96	0.1216	1.29	0.2088	1.14	0.1172	1.14	0.1922	1.20
200	0.2711	0.43	0.3134	0.40	0.0821	0.83	0.1006	1.31	0.1506	0.40	0.1806	0.64	0.1407	0.84	0.1674	0.82
500	0.2276	0.44	0.2502	0.25	0.0728	0.50	0.0818	0.56	0.1322	0.54	0.1485	0.50	0.1205	0.74	0.1339	0.48
1000	0.1938	0.45	0.2125	0.49	0.0632	0.40	0.0702	0.62	0.1151	0.55	0.1288	0.48	0.1031	0.75	0.1140	0.29

Comparing the results of the different codes, one can still notice some discrepancies, especially for the 50-keV incident photons. The deviation of the mean results of each code relative to the general mean value (%) are presented in Figure 24 and Figure 25, for the full-energy peak efficiency and the total efficiency, respectively.

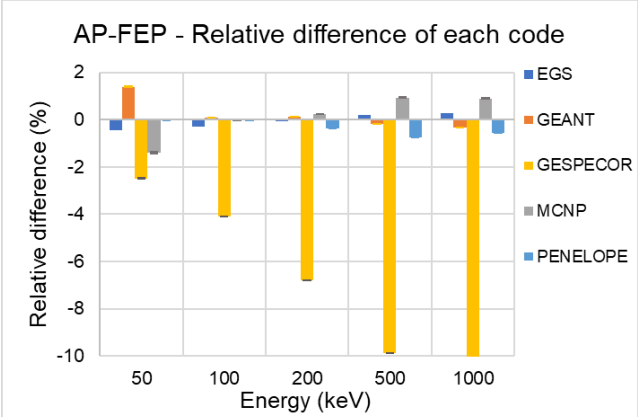

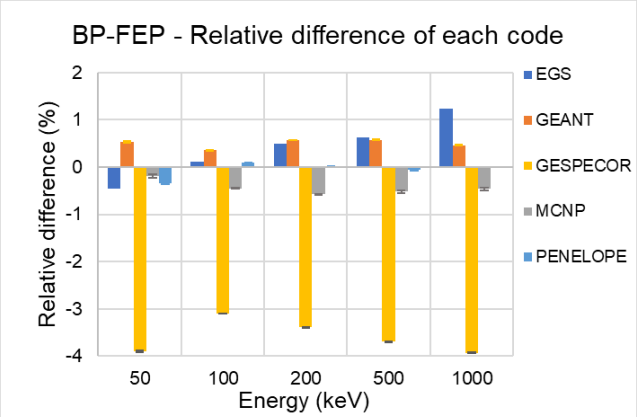

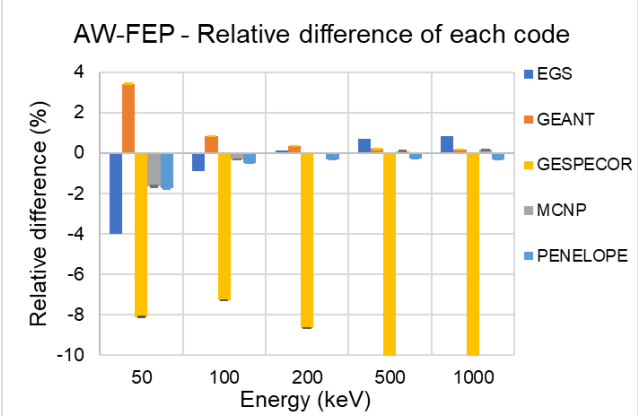

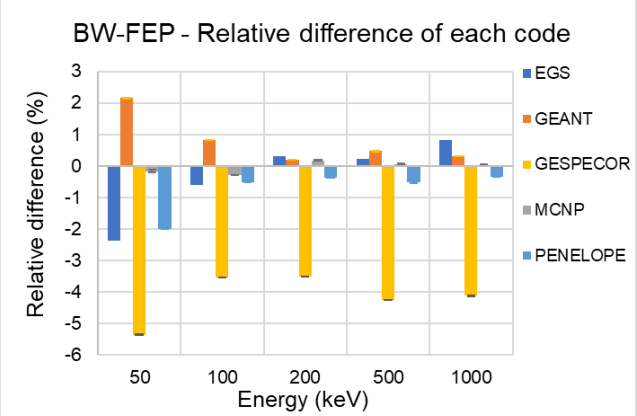

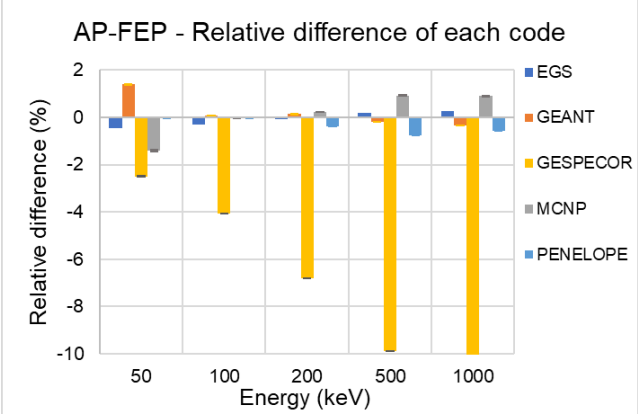

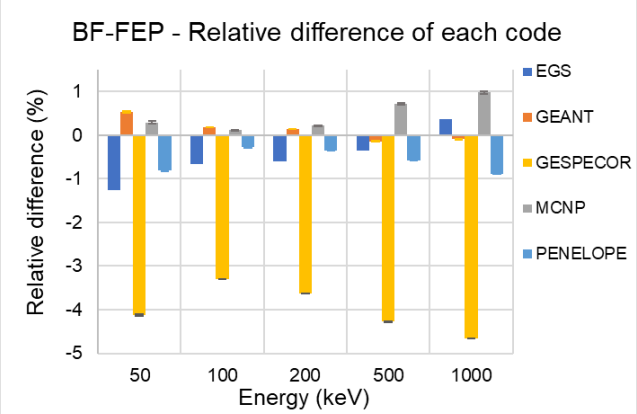

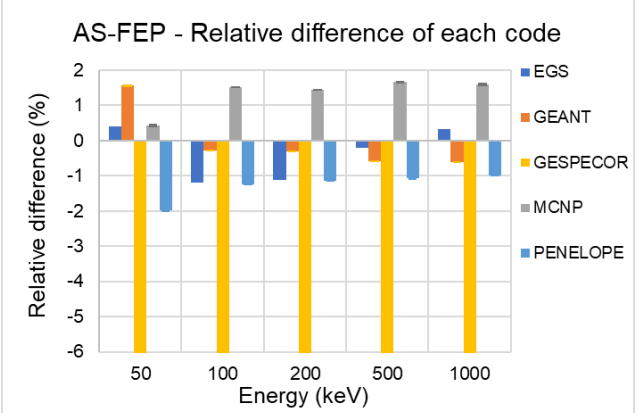

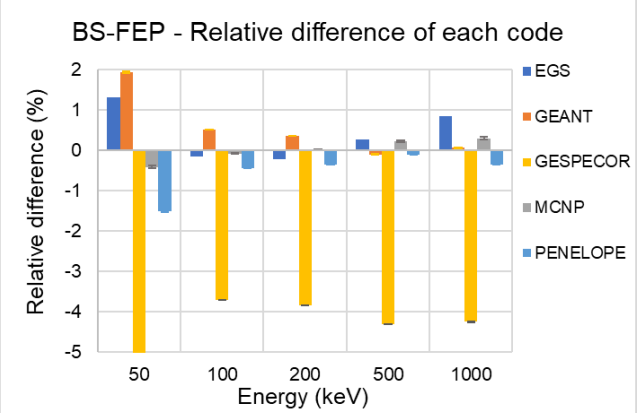

Figure 24: Relative differences (%) between the mean value from each code and the general mean value for the full-energy peak efficiency

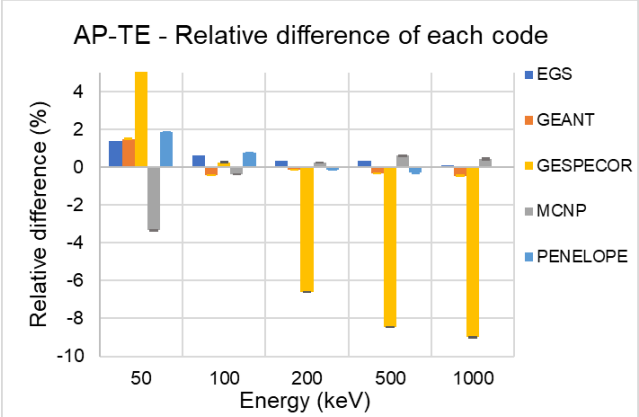

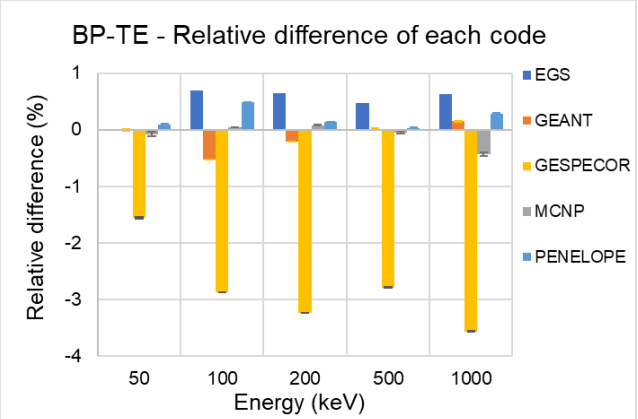

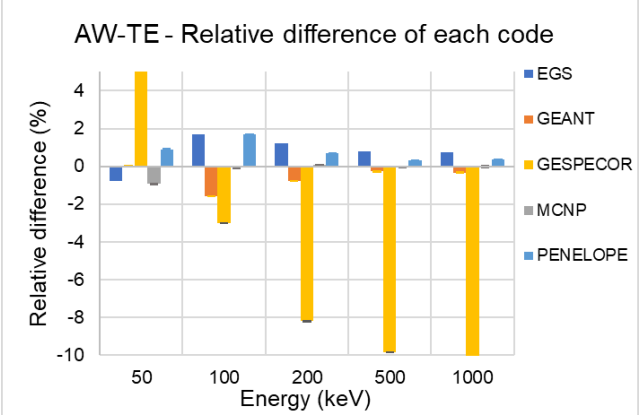

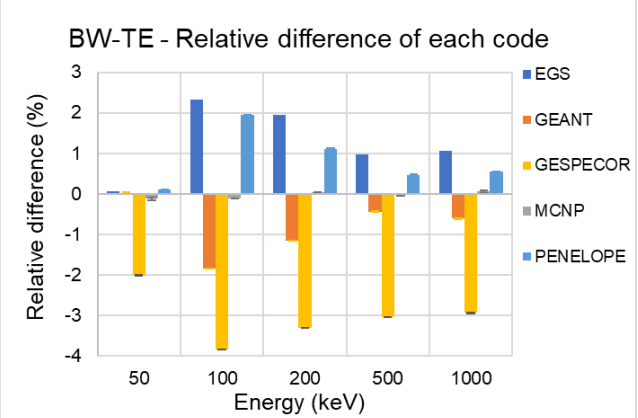

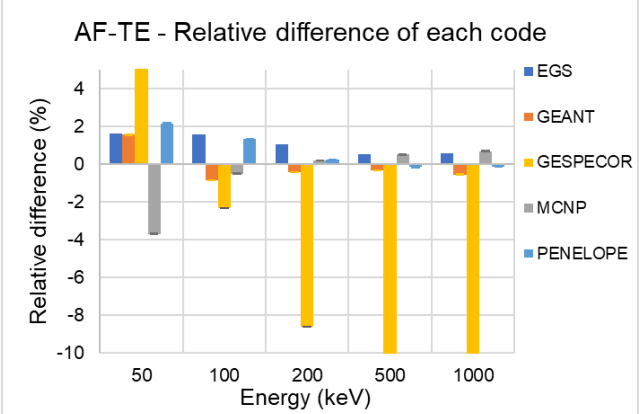

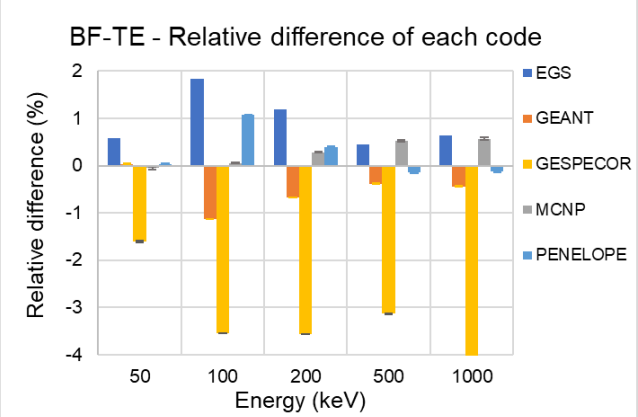

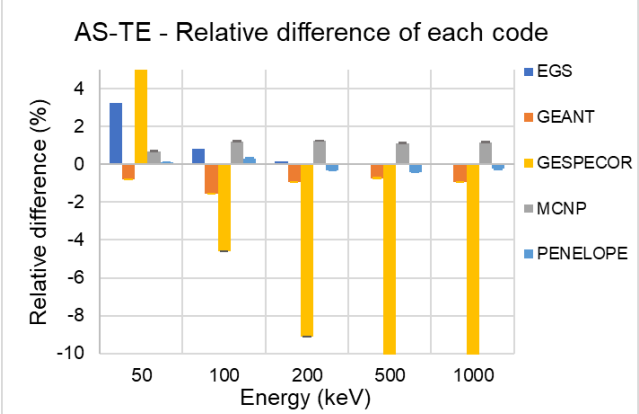

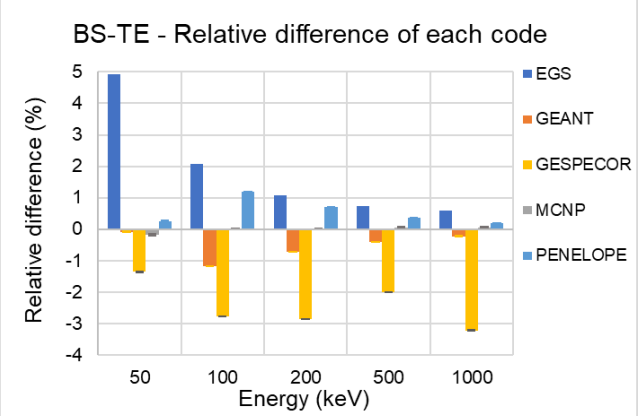

Figure 25: Relative differences (%) between the mean value from each code and the general mean value for the total efficiency

A systematically larger deviation is noted for the code GESPECOR. One possible cause of this discrepancy is the definition of the FEP efficiency, which is applied in standard computations in GESPECOR. It is based on the definition of the peak count rate as the number of counts between the limits L and R, which are the channels with the net count rate equal to 1/10 from the net peak height in the left and right part of the peak, respectively. With this definition, the peak area is equal to 0.9682 from the ideal full peak area in the case of a Gaussian peak. Thus the peak efficiency calculated by GESPECOR is 0.9682 of the ideal peak efficiency which would be obtained considering all pulses belonging to the peak, considered a Gaussian shape.
Thus, to avoid a biased comparison, in a second step, results obtained with GESPECOR were discarded from an additional comparison of relative deviations, as displayed in Figure 26 and Figure 27.

Note: It should be mentioned that despite the dependence of the FEP efficiency on this definition (on the factor 0.9682 or 1, the latter if an ideal Gaussian is used), the self-attenuation, the coincidence-summing and the transfer factor calculated by GESPECOR are independent of the definition of the peak area.

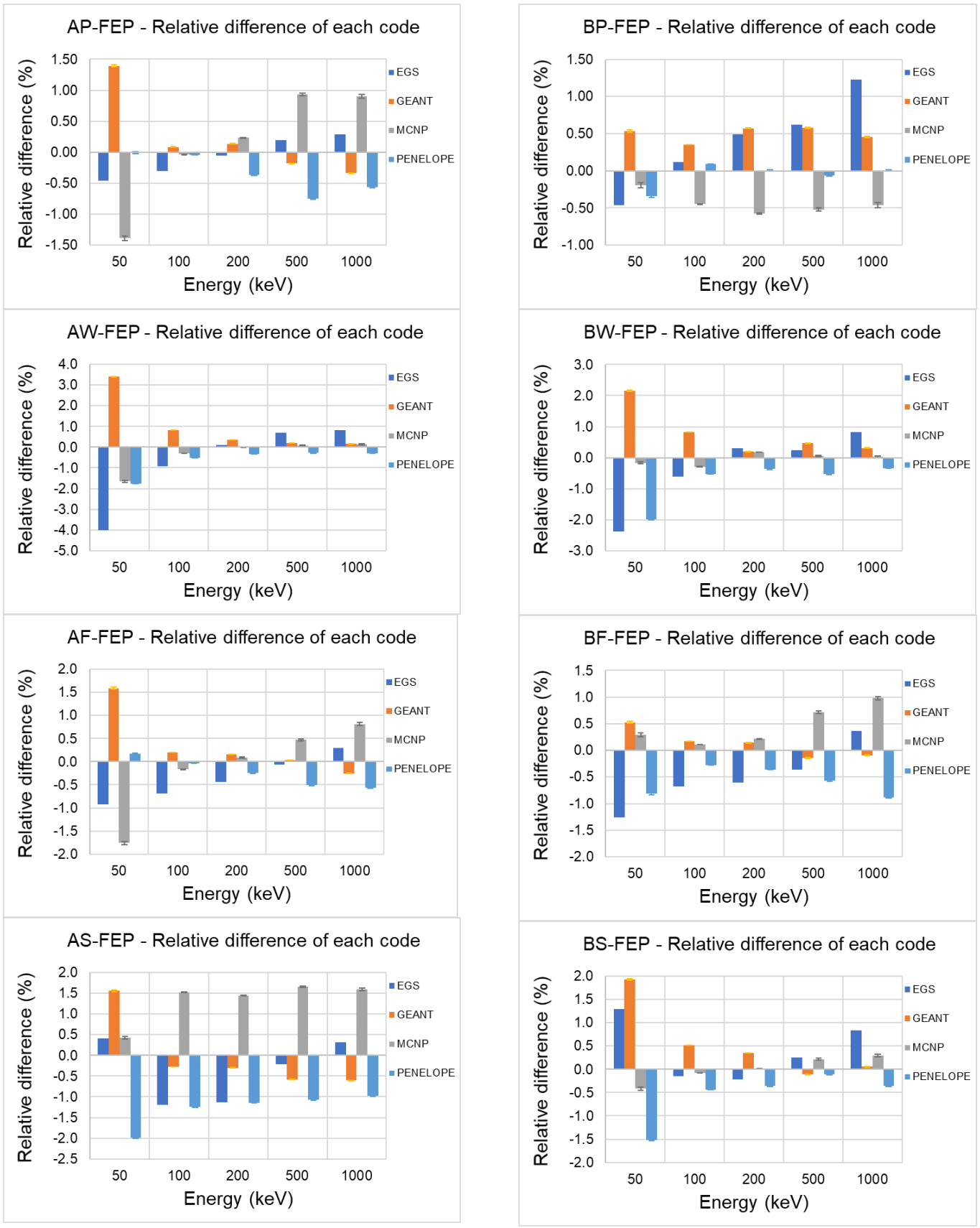

Figure 26: Relative differences (%) between the mean value from each code (except GESPECOR) and the general mean value for the full-energy peak efficiency

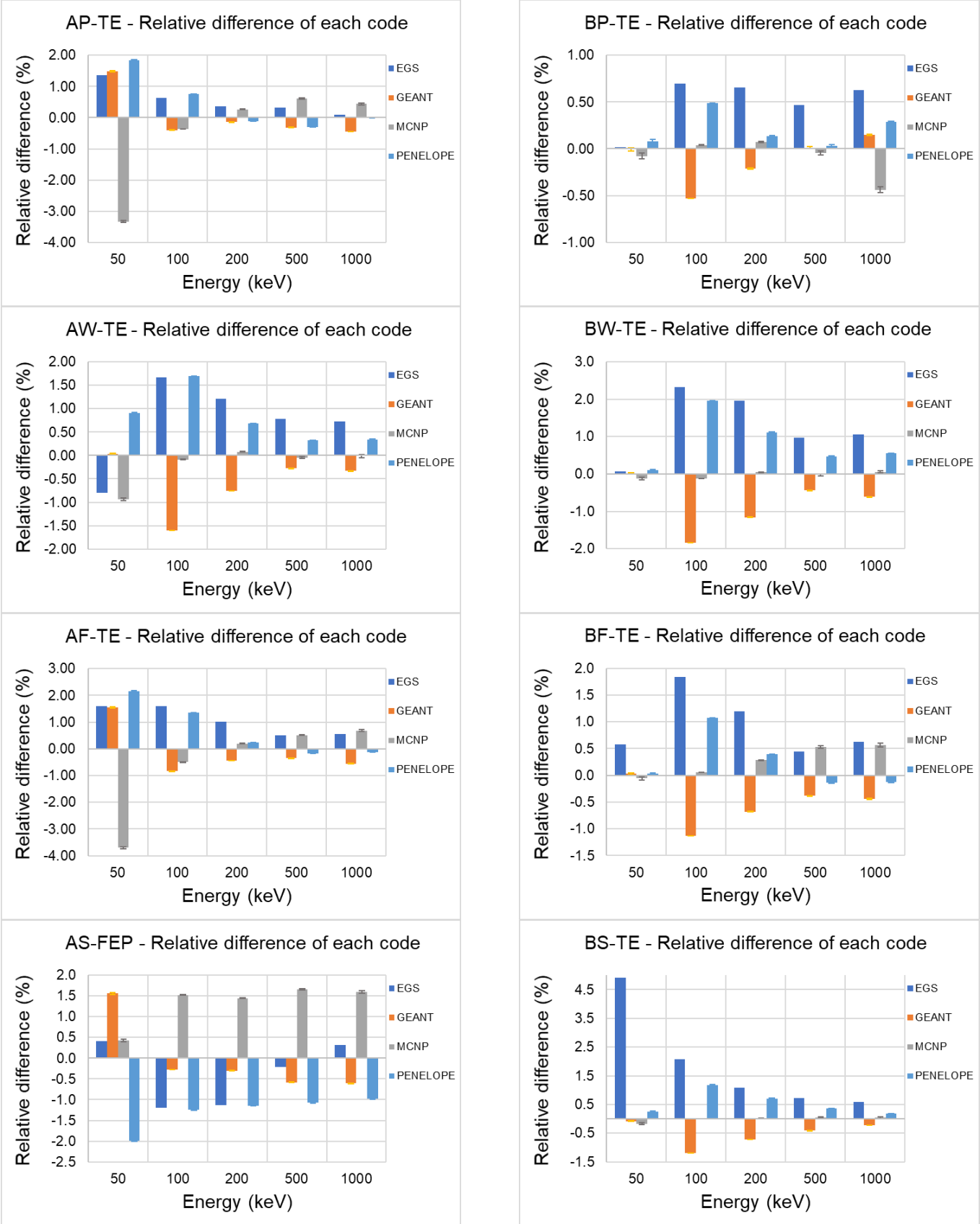

Figure 27: Relative differences (%) between the mean value from each code (except GESPECOR) and the general mean value for the total efficiency

Detailed results are plotted in ANNEX 2 where Figure 31 and Figure 32 provide an overview of the relative deviation of each participant's data from the mean value (%) for each study case. For the FEP efficiencies, each mean value was established from sixteen results, excluding the GESPECOR values and the MCNP results computed without shielding, to obtain a homogeneous set of data. The mean values for the total efficiencies were obtained using only the twelve most consistent data sets.

For the FEP, It can be noted that, with the exception of the GESPECOR results, the discrepancies of which have been explained above, and of the water sample at 50 keV, all relative differences generally remain within ±2 %. The same tendency is observed for the TE, where relative differences higher than 2 % are due to the data sets that were excluded to establish the mean value: these discrepancies may be due to an erroneous definition of the total efficiency depending on the code user.

Another way to examine the results is to calculate the quadratic sum of relative deviations of the five energies for each geometry as follows:

$$RDi = \sum_E \left(\frac{(FEPE\ (E)\ or\ TE(E)) - MV(E)}{MV(E)} \cdot 100\right)^2 \text{ (E = 50 keV, 100 keV, 200 keV, 500 keV, 1000 keV)}$$

where

$$MV(E) = \frac{\sum_i (FEPE(E) or\ TE(E))}{N}$$

N being the number of data points used to compute the mean value (16 for the FEPE and 12 for the TE).

These values are presented in Table 13 for the FEPE and in Table 14 for the TE, where the last line is the sum of the eight individual study cases. The colors refer to a specific code (yellow = GEANT, blue = GESPECOR, pink = PENELOPE, green = MCNP, orange = EGSnrc).

Table 13: Quadratic sum of the relative deviations for the FEP efficiency calculations

Participant	1	2	3	4	5	6	7	8	9	10	11	12	13	14	15	16	17	18	19
AP	1.65	1.55	10.01	1.53	300	301	0.97	1.52	0.12	1.66	2.42	3.68	0.09	114.33	0	0	109.29	0.96	0.30
BP	0.46	0.82	0.28	0.40	43	44	0.24	1.28	0.30	0.53	0.26	0.92	0.63	0.29	10383	10366	2.57	8490	1.26
AW	5.32	6.62	5.22	5.55	2223	2378	4.15	5.73	2.59	4.21	2.72	2.45	3.44	5.26	6765	6753	6.50	6651	5.30
BW	7.33	6.79	6.06	9.23	48	57	5.13	6.42	4.83	5.47	3.90	1.64	3.99	6.96	6946	6929	8.50	6855	8.77
AF	1.37	1.65	8.42	2.60	3673	3730	2.66	4.33	1.10	3.43	2.65	3.85	1.13	85.29	8444	8433	85.72	8411	3.89
BF	2.48	2.50	2.30	2.63	51	57	1.23	1.84	1.31	1.44	1.31	1.52	1.34	4.45	8697	8675	4.25	8669	5.33
AS	4.43	4.43	3.36	4.82	1608	1532	0.39	0.92	0.95	0.34	0.42	2.06	14.67	5.60	11363	11350	4.55	11257	12.54
BS	2.67	4.87	1.69	3.37	33	37	1.52	2.52	1.46	1.52	2.89	0.93	1.43	2.00	10964	10944	2.54	10907	28.69
QUADRATIC SUM	*25.71*	*29.23*	*37.33*	*30.12*	*7979*	*8135*	*16.30*	*24.56*	*12.65*	*18.60*	*16.57*	*17.05*	*26.72*	*224.17*	*63562*	*63451*	*223.93*	*61241*	*66.07*

Table 14: Quadratic sum of the relative deviations for the total efficiency calculations

Participant	1	2	3	4	5	6	7	8	9	10	11	12	13	14	15	16	17	18	19
AP	0.52	1.16	5.85	0.59	3779	3873	2.84	2.55	0.90	2.07	3.11	2.31	0.42	79.23	11211	11201	70.91	11239	0.79
BP	0.46	0.82	0.28	0.40	43	44	0.24	1.28	0.30	0.53	0.26	0.92	0.63	0.29	10383	10366	2.57	8490	1.26
AW	5.32	6.62	5.22	5.55	2223	2378	4.15	5.73	2.59	4.21	2.72	2.45	3.44	5.26	6765	6753	6.50	6651	5.30
BW	7.33	6.79	6.06	9.23	48	57	5.13	6.42	4.83	5.47	3.90	1.64	3.99	6.96	6946	6929	8.50	6855	8.77
AF	1.37	1.65	8.42	2.60	3673	3730	2.66	4.33	1.10	3.43	2.65	3.85	1.13	85.29	8444	8433	85.72	8411	3.89
BF	2.48	2.50	2.30	2.63	51	57	1.23	1.84	1.31	1.44	1.31	1.52	1.34	4.45	8697	8675	4.25	8669	5.33
AS	4.43	4.43	3.36	4.82	1608	1532	0.39	0.92	0.95	0.34	0.42	2.06	14.67	5.60	11363	11350	4.55	11257	12.54
BS	2.67	4.87	1.69	3.37	33	37	1.52	2.52	1.46	1.52	2.89	0.93	1.43	2.00	10964	10944	2.54	10907	28.69
QUADRATIC SUM	*24.59*	*28.83*	*33.17*	*29.18*	*11458*	*11708*	*18.17*	*25.59*	*13.43*	*19.02*	*17.26*	*15.68*	*27.05*	*189.08*	*74772*	*74651*	*185.55*	*72479*	*66.57*

In general, it appears that the efficiencies calculated with GEANT4 and PENELOPE are the most consistent and provide overall the smallest relative deviations from the mean values.

6. Training material

The goal of the present exercise was to prepare some practical examples to calculate detection efficiencies for new users of Monte Carlo simulation tools. For each generalist code, sharing the experience of several participants made it possible to agree on the determination of input files and to identify some possible difficulties to avoid their incorrect use.
The comparison between the efficiency results calculated with different codes showed satisfactory agreement, with about 1 %-2 % maximum relative deviation. This leads to the conclusion that the geometry models used by the participants are reliable and can be distributed as examples.
Consequently, as an output of the exercise, practical material is made available at the ICRM GSWG web page (http://www.lnhb.fr/icrm_gs_wg/icrm_gs_wg_benchmarks/), so that new users may train themselves. For each of the generalist codes (GEANT4, MCNP, PENELOPE and EGSnrc), the distributed package includes:

i) the specific input files as prepared and agreed by different users, for the eight study cases;
ii) the calculation results, including the mean values and associated standard deviations;
iii) in addition, specific advices and warning to properly run the codes as derived from the experience of the users.

These selected simple geometries should be used as training material for testing that the efficiency calculation results obtained by novices in Monte Carlo simulation are reliable within 1 %-2 %.

7. Conclusion

As already highlighted in a previous exercise conducted under the auspices of the ICRM GSWG (Vidmar *et al*., 2008), there are different approaches either in the implementation of the physical interaction processes or in the practical definition of the efficiencies which prevent achieving full comparisons between the Monte Carlo codes. In the present exercise, the aim was to agree on eight selected study cases, with well defined simple geometries and to run different Monte Carlo codes to derive the full-energy peak and total efficiencies associated to different energies. In most of the cases, the relative standard deviations of individual results from the mean value are less than 1%. As expected, some larger deviations may be seen at 50 keV for the “Detector A” geometries and for other low efficiency cases: however, this should be compared to the uncertainty associated to the simulation results, which are significantly higher for low efficiencies. In the calculation conditions used by most of the participants, the simulations were performed with 10^7 initial particles: an efficiency value of 2 % means that 2 000 interactions occur in the detector, which consequently induces a high relative statistical uncertainty of 3.2 %. This stresses the influence of the number of particles used for the simulation, which must be large enough to obtain relevant results for low efficiencies. The goal of the present exercise was to provide some practical examples for new users, which was effectively achieved. The input files for each code and the eight study cases were prepared and agreed by different users. In the same way, the calculation results, including the mean values and associated standard deviations are available. It is wished that this material will be useful for beginners in the use of Monte Carlo codes for gamma-ray spectrometry. In addition, a next step is planned, which will be dedicated to the use of such Monte Carlo codes for the calculation of coincidence corrections.

8. References

Agostinelli S., et al., 2003. *GEANT4-a simulation toolkit.* Nuclear Instruments and Methods A 506, 250-303.

Allison J., et al., 2006. *Geant4 developments and applications*. IEEE Trans. Nucl. Sci., 53, 270-278.

Allison, J., et al., 2016. *Recent developments in Geant4.* Nuclear Instruments and Methods in Phys. Res. A835, 186-225. (https://doi.org/10.1016/j.nima.2016.06.125)

Briesmeister J.C., (Ed.), 2000. *MCNP-A General Monte Carlo N-Particle Transport Code, Version 4C*. Los Alamos National Laboratory Report LA-13709-M, Los Alamos.

Chirosca, A., Suvaila, R., Sima, O., 2013. *Monte Carlo simulation by GEANT 4 and GESPECOR of in situ gamma-ray spectrometry measurements.* Applied Radiation and Isotopes 81, 87-91.

Cook, A. J., 1983. *Mortran3 user's guide*. SLAC Computation Research Group Report CGTM-209.

Cornejo Díaz, N., Jurado Vargas, M., 2008. *DETEFF: An improved Monte Carlo computer program for evaluating the efficiency in coaxial gamma-ray detectors.* Nuclear Instruments and Methods in Physics Research A, 586, 204-210.

EGS, 2019. http://nrc-cnrc.github.io/EGSnrc/

GEANT4, 2019. http://geant4.web.cern.ch/

Goorley, J.T. et al., 2013. *Initial MCNP6 Release Overview - MCNP6 version 1.0* - LA-UR-13-22934.

Helmer, R. G., Nica, N., Hardy, J. C., Jacob, V. E., 2004. *Precise efficiency calibration of an HPGe detector up to 3.5 MeV, with measurements and Monte Carlo calculations.* Applied Radiation and Isotopes 60, 173-177.

Hurtado, S., García-Leon, M., García-Tenorio, R., 2004. *GEANT4 code for simulation of a germanium gamma-ray detector and its application to efficiency calibration.* Nuclear Instruments and Methods A 518, 764-774.

Lépy, M.-C., Thiam, C., Anagnostakis, M., Galea, R., Gurau, D., Hurtado, S., Karfopoulos, K., Liang, J., Liu, H., Luca, A., Mitsios, I., Potiriadis, C., Savva, M. I., Tran, T.T., Thomas, V., Townson, R.W., Vasilopoulou, T., Zhang, M., *A benchmark for Monte Carlo simulation in gamma-ray spectrometry.* Applied Radiation and Isotopes, 2020, 154, 108850

MCNP, 2019. https://mcnp.lanl.gov/

Peyres, V., García-Toraño, E., 2007. *Efficiency calibration of an extended-range Ge detector by a detailed Monte Carlo simulation*. Nuclear Instruments and Methods in Physics Research A580, 296-298.

García-Toraño, E., Pozuelo, M., Salvat, F., 2005. *Monte Carlo calculations of coincidence-summing corrections for volume sources in gamma-ray spectrometry with Ge detectors*. Nuclear Instruments and Methods in Physics Research A544, 577-583.

Kawrakow, I., 2000. *Accurate condensed history Monte Carlo simulation of electron transport. I. EGSnrc, the new EGS4 version*. Medical physics 27, 485-498.

Nelson, W. R., Hirayama, H., Rogers, D. W. O., 1985. *The EGS4 code system.* Report SLAC-265.

Salvat, F., 2015. *PENELOPE-2014: A code System for Monte Carlo Simulation of Electron and Photon Transport.* OECD/NEA Data Bank, NEA/NSC/DOC(2015)3. Issy-les-Moulineaux, France. Available from ⟨http://www.nea.fr/lists/penelope.html⟩

Salvat, F., Fernández-Varea, J. M., 2009. *Overview of physical interaction models for photon and electron transport used in Monte Carlo codes.* Metrologia 46, S112–S138.

Sima, O., Arnold, D., Dovlete, C., 2001. *GESPECOR – a versatile tool in gamma-ray spectrometry*. Journal of Radioanalytical and Nuclear Chemistry 248, 359-364.

Sima, O., 2012. *Efficiency calculation of gamma detectors by Monte Carlo methods.* in Encyclopedia of Analytical Chemistry, Online, Wiley

Vidmar, T., Aubineau-Lanièce, I., Anagnostakis, M., Arnold, D., Brettner-Messler, R., Budjas, D., Capogni, M., Dias, M.S., De-Geer, L.-E., Fazio, A., Gasparro, J., Hult, M., Hurtado, S., Jurado Vargas, M., Laubenstein, M., Lee, K.B., Lee, Y.-K., Lépy, M.-C., Maringer, F.-J., Medina Peyres, V., Mille, M., Morales, M., Nour, S., Plenteda, R., Rubio Montera, M.P., Sima, O., Tomei, C., Vidmar, G., 2008. *An intercomparison of Monte Carlo codes used in gamma-ray spectrometry.* Applied Radiation and Isotopes 66, 764-768.

Vidmar, T., Capogni, M., Hult, M., Hurtado, S., Kastlander, J., Lutter, G., Lépy, M.-C., Martinkovič, J., Ramebäck, H. , Sima, O., Tzika, F., Vidmar, G., 2014. *Equivalence of computer codes for calculation of coincidence summing correction factors*. Applied Radiation and Isotopes 87, 336–341.

ANNEX 1: Details of the geometrical characteristics

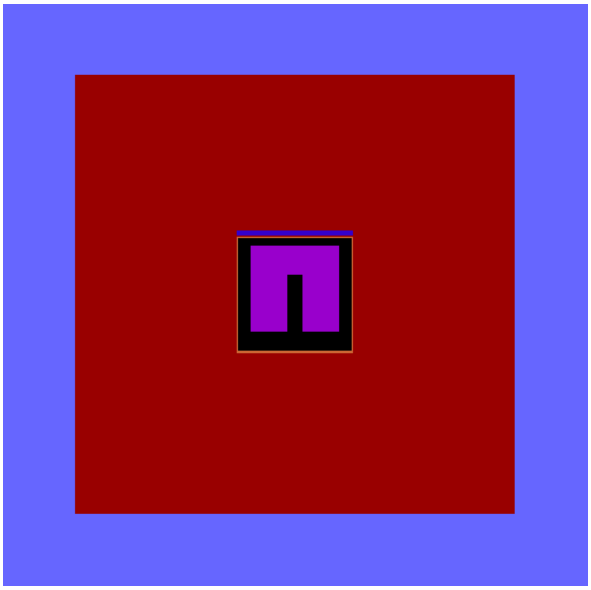

Figure 28: Detector in lead shielding

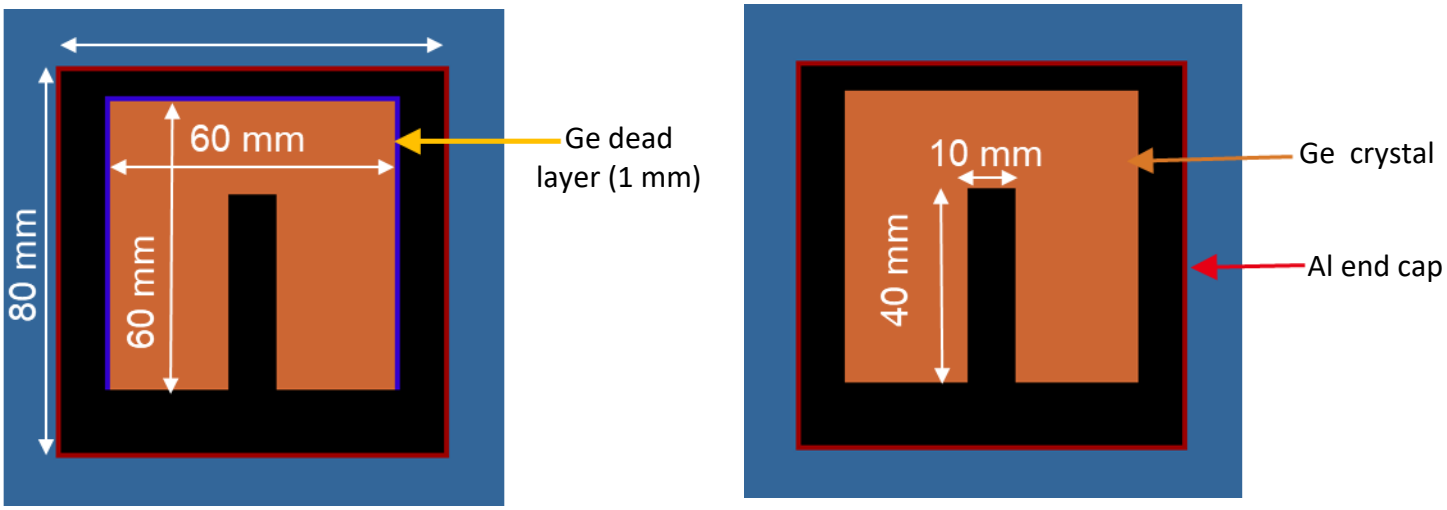

Figure 29: Dimensions of P-type detector (A: left) and N-type detector (B: right)

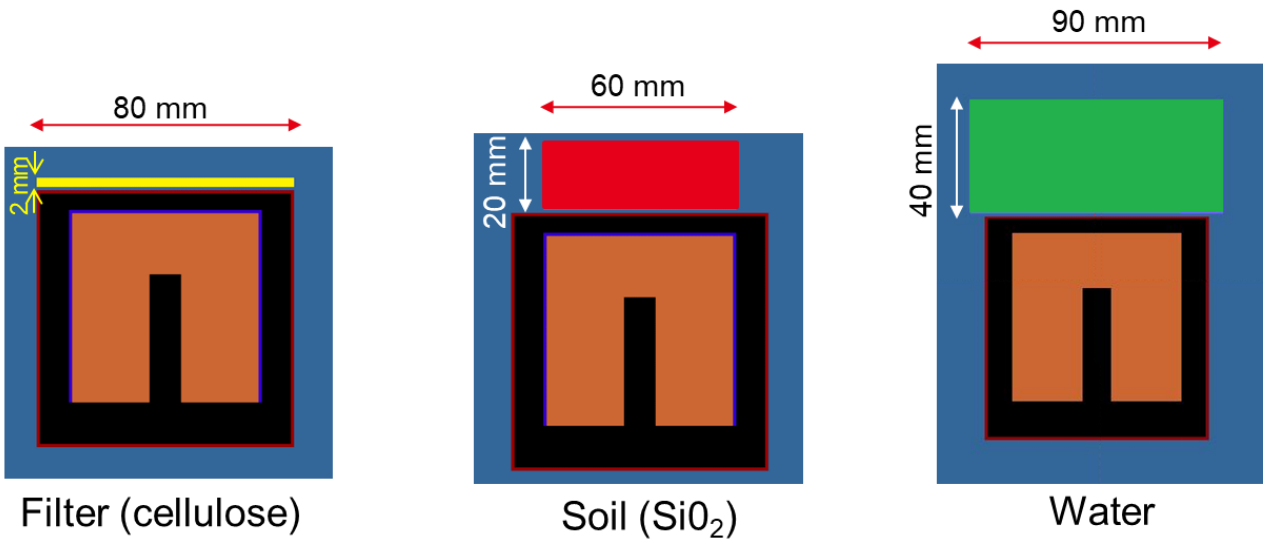

Figure 30: Volume geometries

ANNEX 2: Relative deviations of individual results

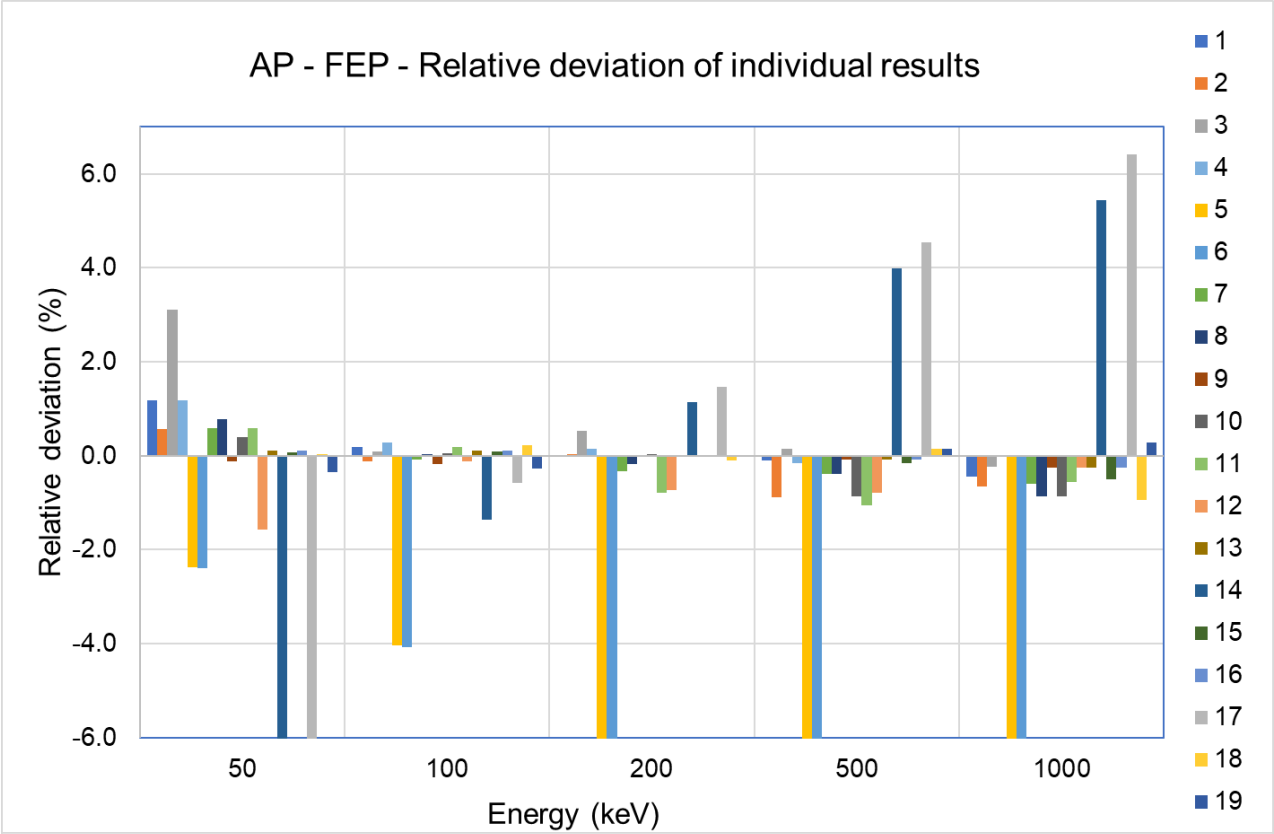

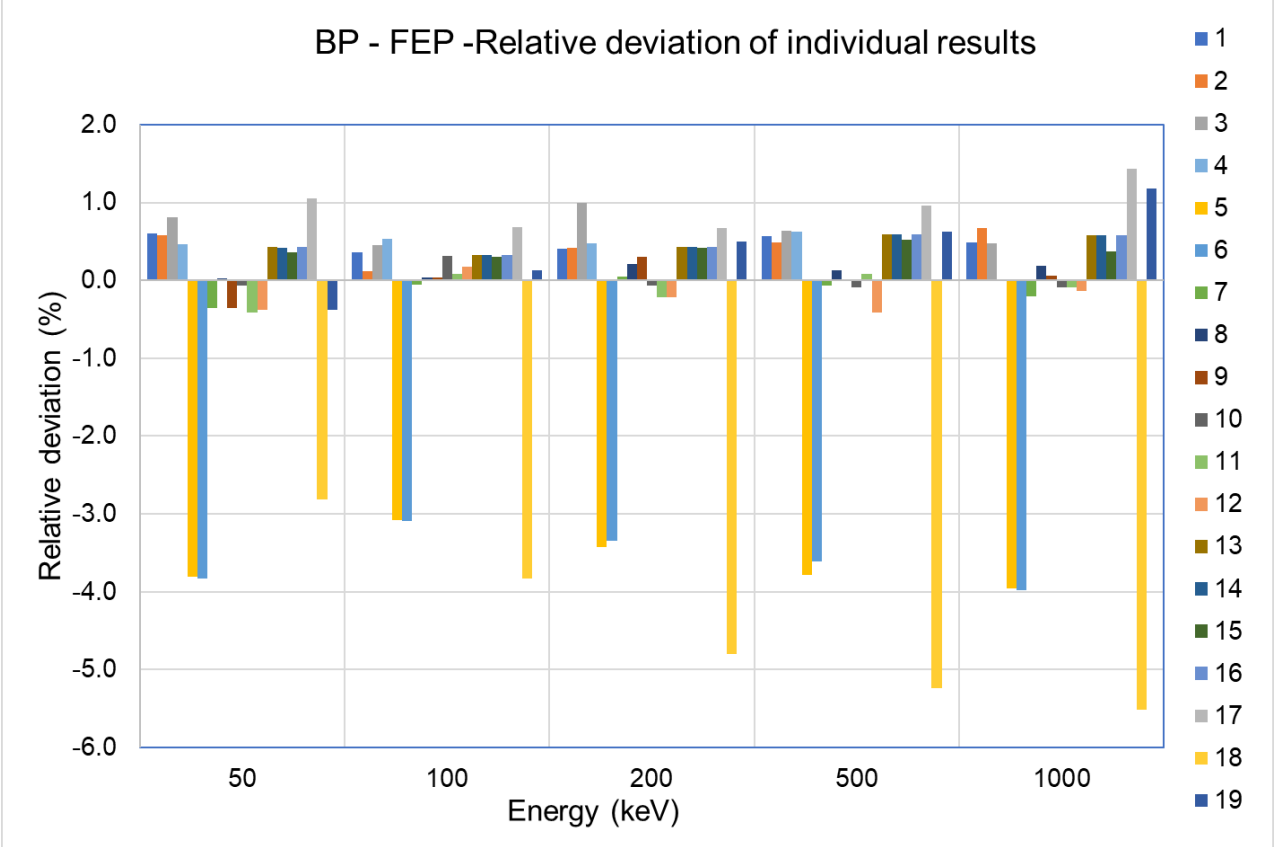

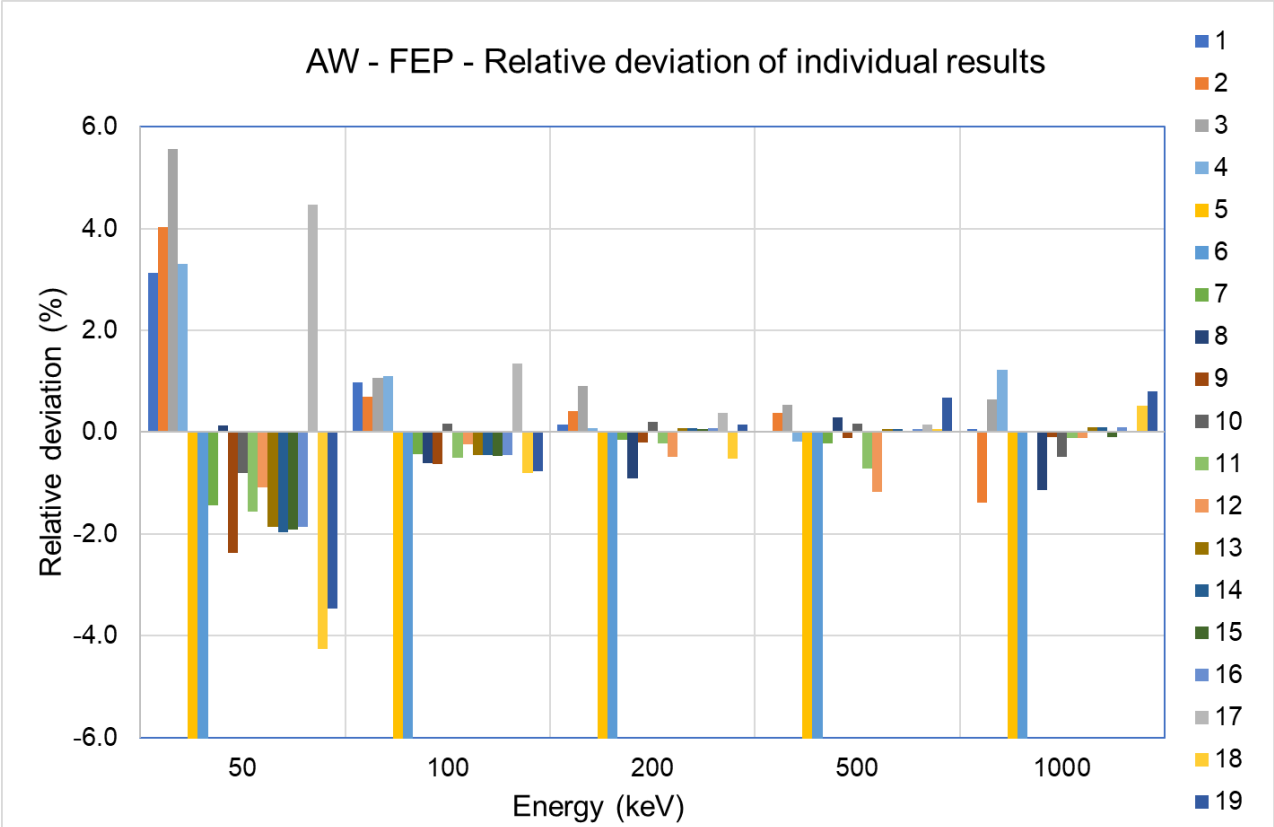
AW - FEP - Relative deviation of individual results
Relative deviation (%)
6.0
4.0
2.0
0.0
-2.0
-4.0
-6.0
50
100
200
500
1000
Energy (keV)
1
2
3
4
5
6
7
8
9
10
11
12
13
14
15
16
17
18
19

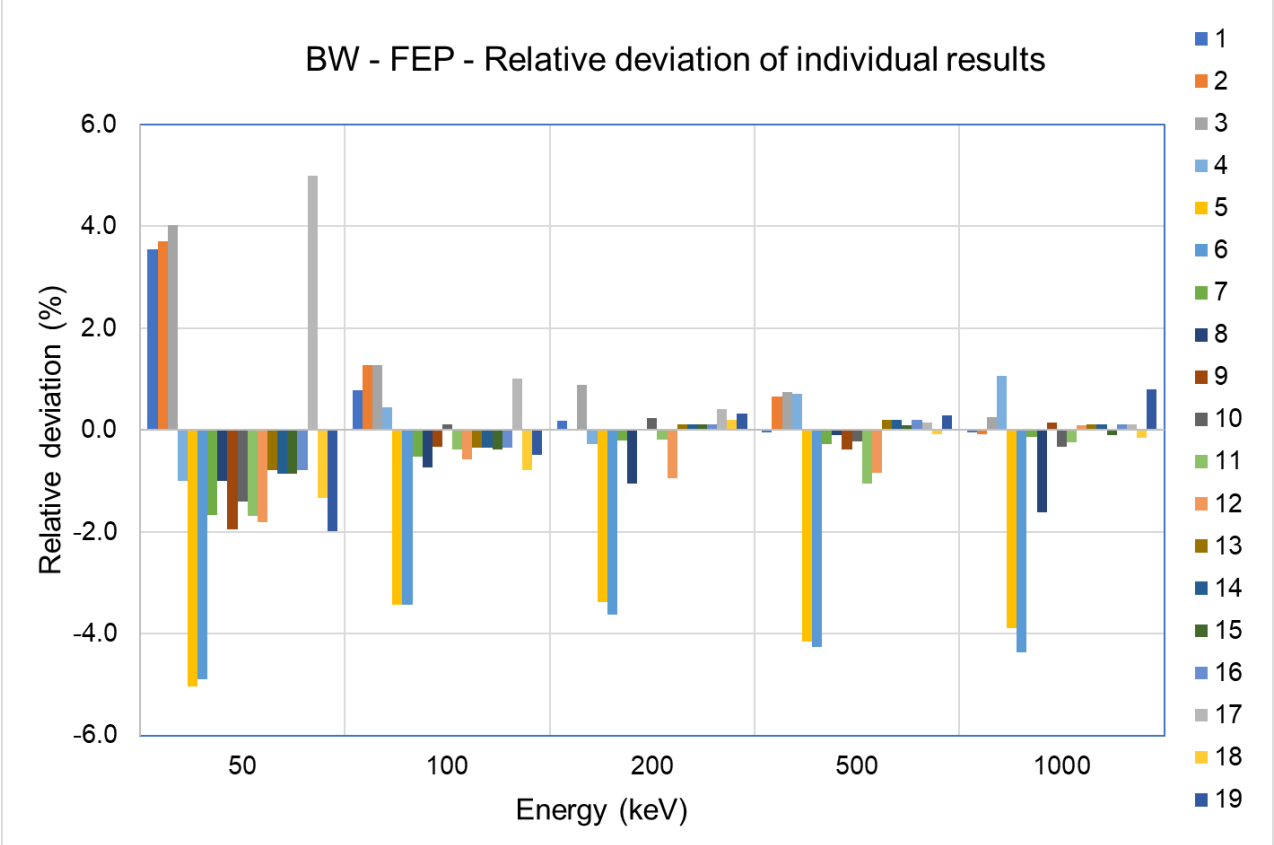
BW - FEP - Relative deviation of individual results
Relative deviation (%)
6.0
4.0
2.0
0.0
-2.0
-4.0
-6.0
50
100
200
500
1000
Energy (keV)
1
2
3
4
5
6
7
8
9
10
11
12
13
14
15
16
17
18
19

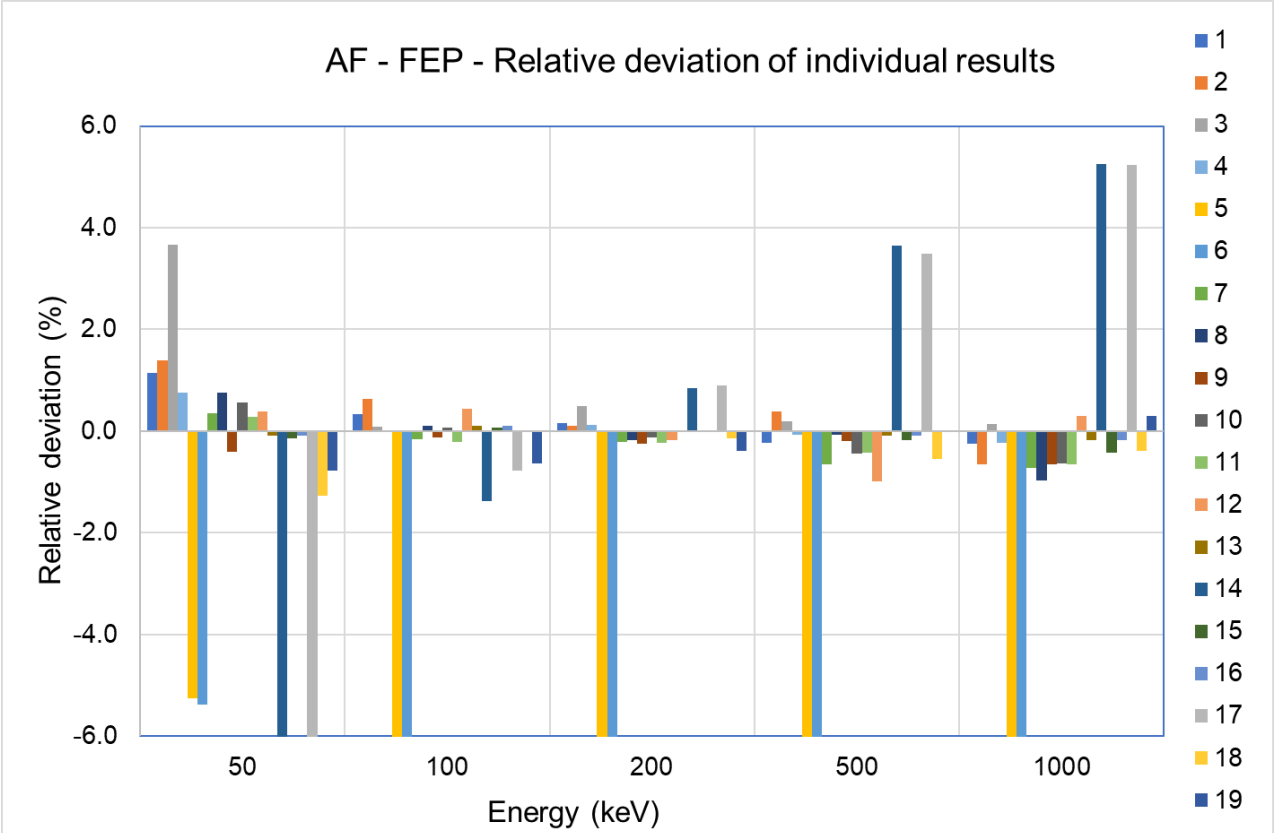
AF - FEP - Relative deviation of individual results
Relative deviation (%)
6.0
4.0
2.0
0.0
-2.0
-4.0
-6.0
50
100
200
500
1000
Energy (keV)
1
2
3
4
5
6
7
8
9
10
11
12
13
14
15
16
17
18
19

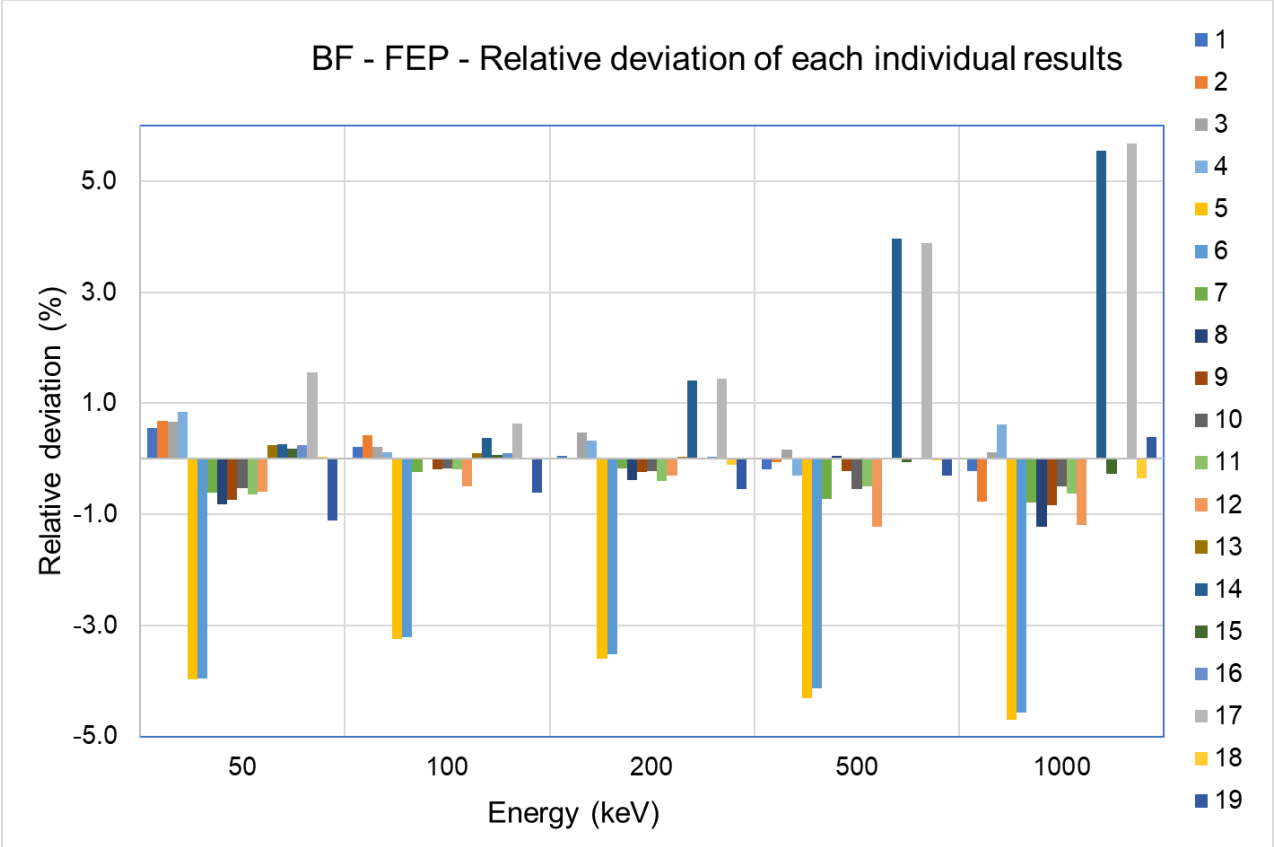
BF - FEP - Relative deviation of each individual results
Relative deviation (%)
5.0
3.0
1.0
-1.0
-3.0
-5.0
50
100
200
500
1000
Energy (keV)
1
2
3
4
5
6
7
8
9
10
11
12
13
14
15
16
17
18
19

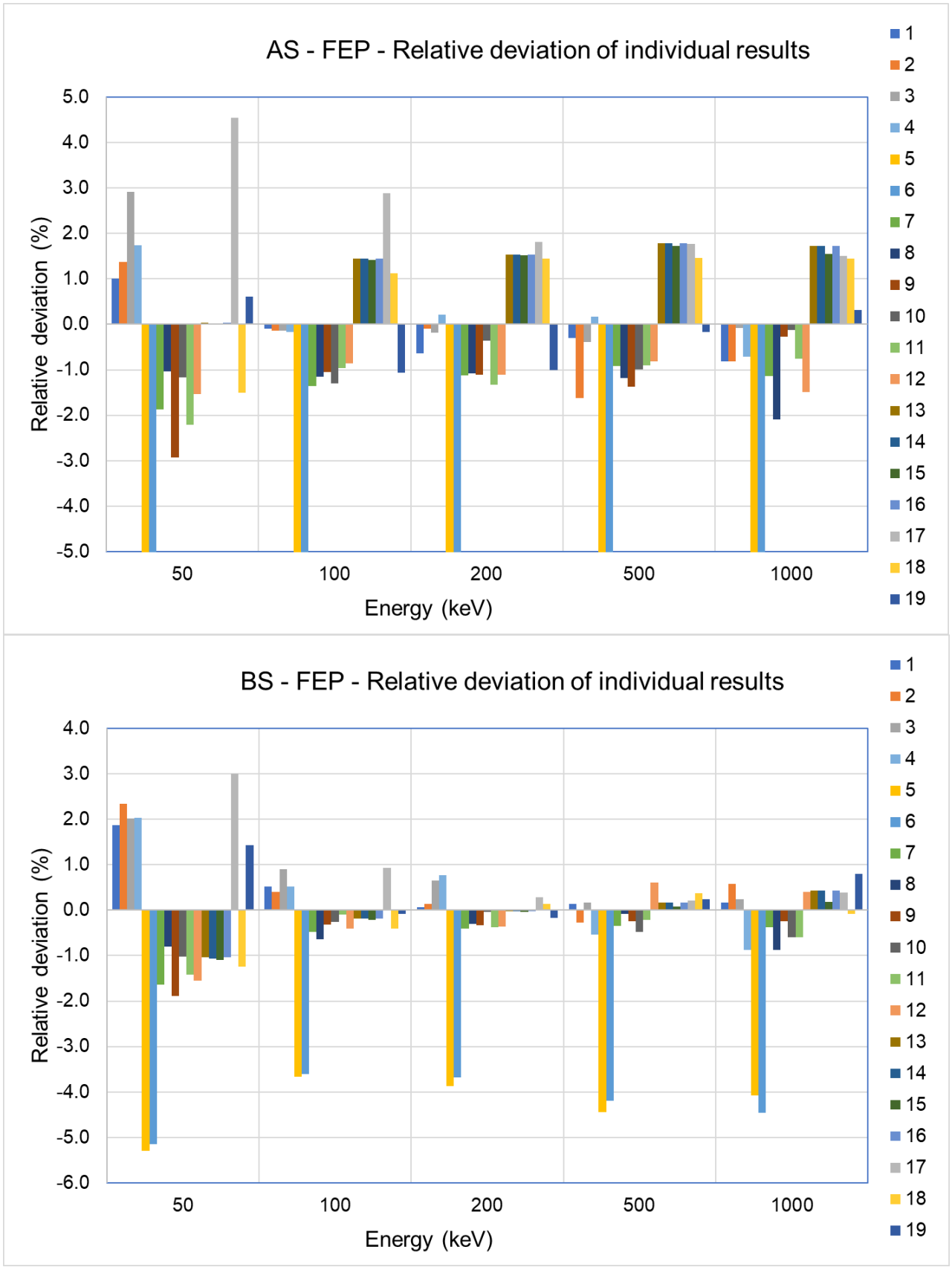

Figure 31 : Deviation of individual results relative to the mean value (%) for the FEP efficiencies

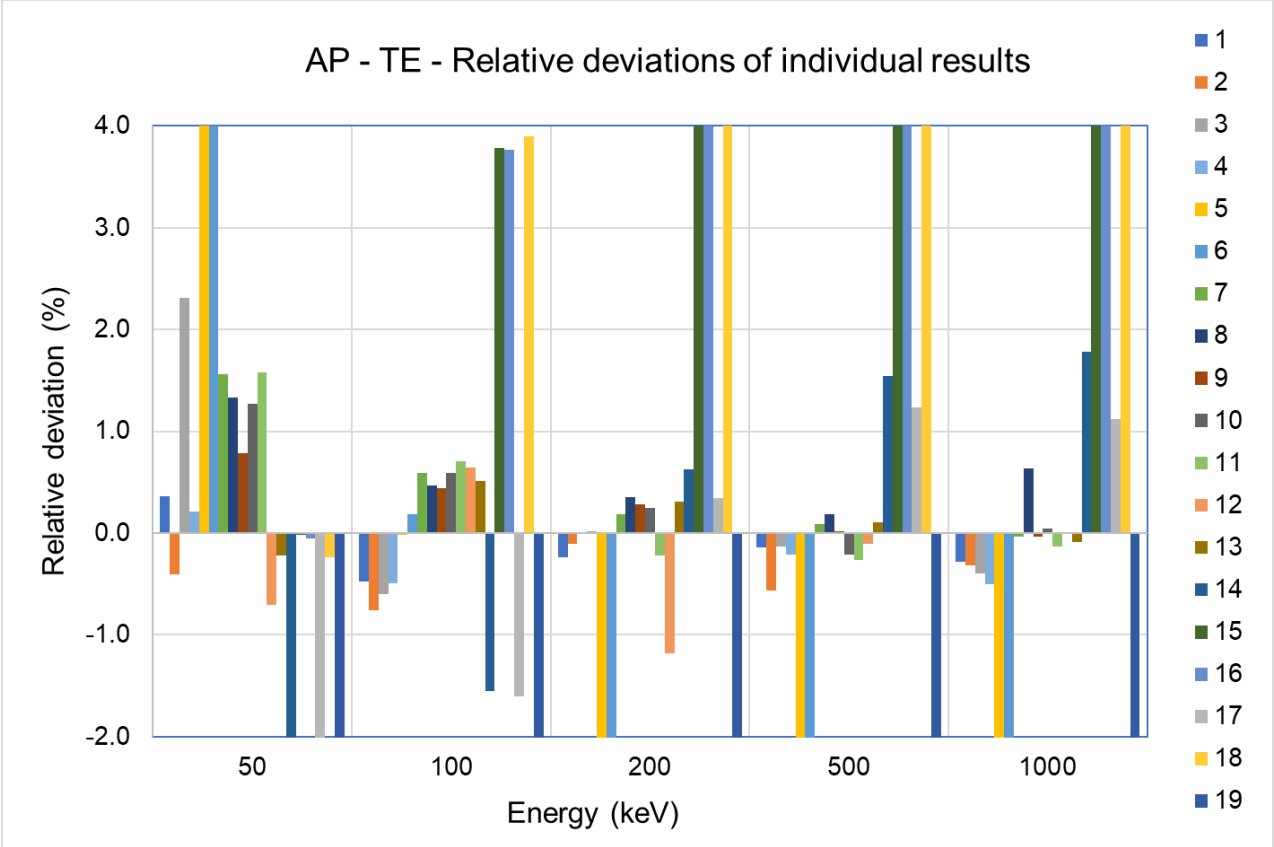
AP - TE - Relative deviations of individual results
Relative deviation (%)
4.0
3.0
2.0
1.0
0.0
-1.0
-2.0
50
100
200
500
1000
Energy (keV)
1
2
3
4
5
6
7
8
9
10
11
12
13
14
15
16
17
18
19

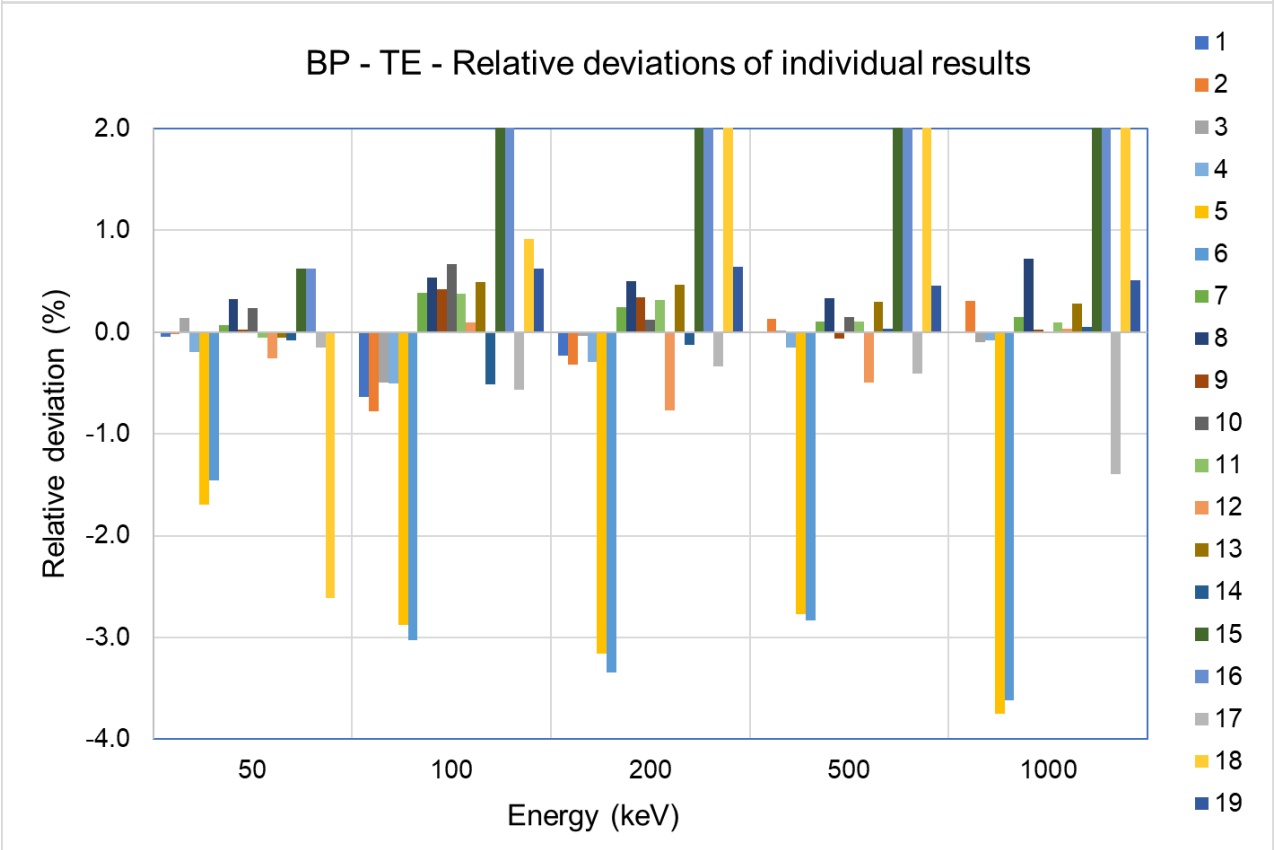
BP - TE - Relative deviations of individual results
Relative deviation (%)
2.0
1.0
0.0
-1.0
-2.0
-3.0
-4.0
50
100
200
500
1000
Energy (keV)
1
2
3
4
5
6
7
8
9
10
11
12
13
14
15
16
17
18
19

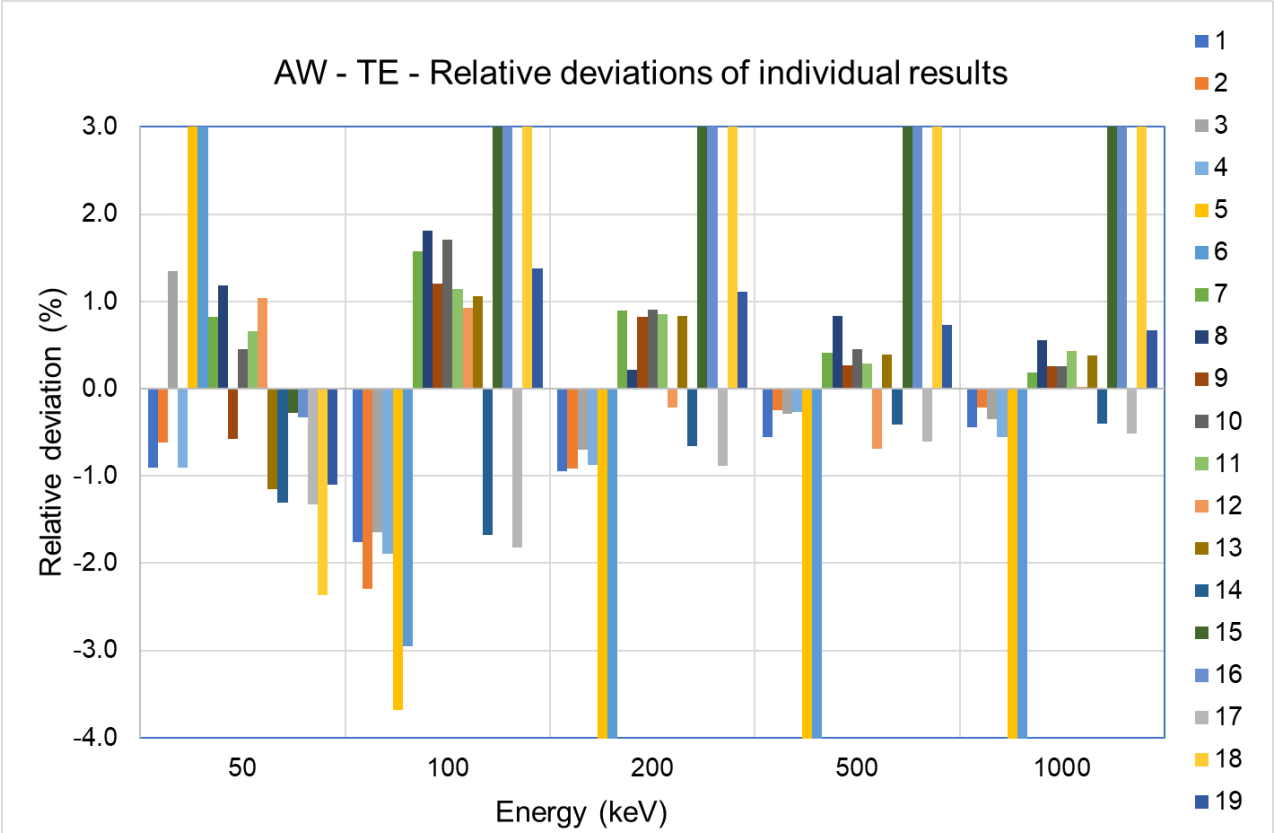
AW - TE - Relative deviations of individual results
Relative deviation (%)
3.0
2.0
1.0
0.0
-1.0
-2.0
-3.0
-4.0
50
100
200
500
1000
Energy (keV)
1
2
3
4
5
6
7
8
9
10
11
12
13
14
15
16
17
18
19

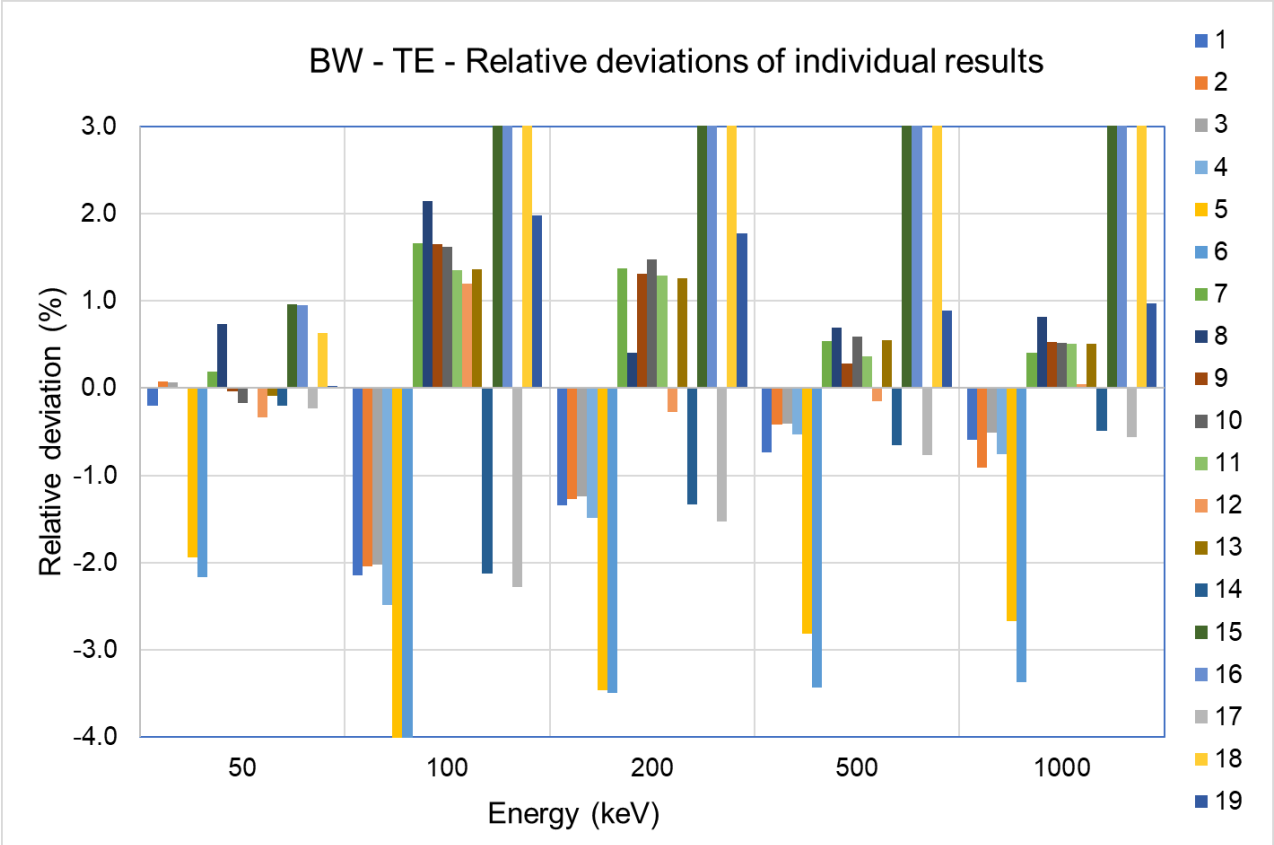
BW - TE - Relative deviations of individual results
Relative deviation (%)
3.0
2.0
1.0
0.0
-1.0
-2.0
-3.0
-4.0
50
100
200
500
1000
Energy (keV)
1
2
3
4
5
6
7
8
9
10
11
12
13
14
15
16
17
18
19

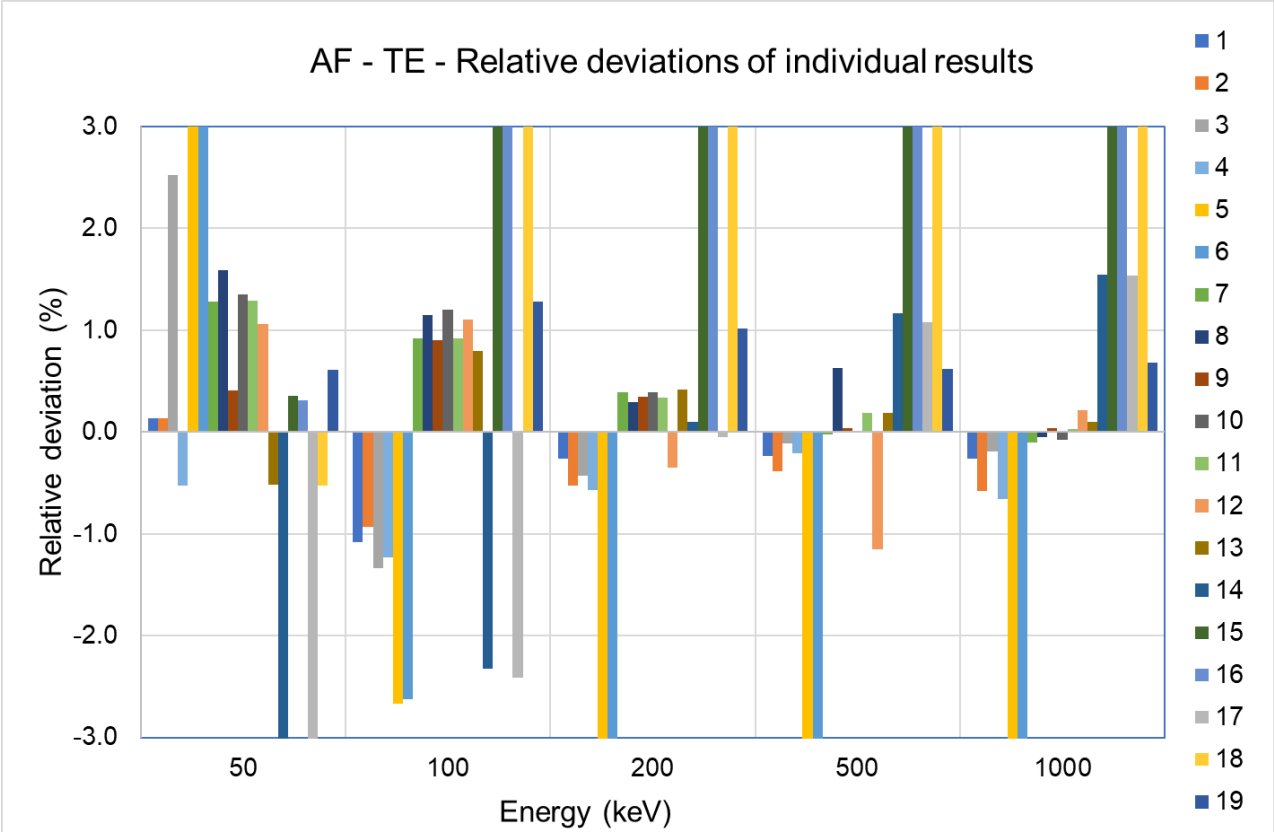
AF - TE - Relative deviations of individual results
Relative deviation (%)
3.0
2.0
1.0
0.0
-1.0
-2.0
-3.0
50
100
200
500
1000
Energy (keV)
1
2
3
4
5
6
7
8
9
10
11
12
13
14
15
16
17
18
19

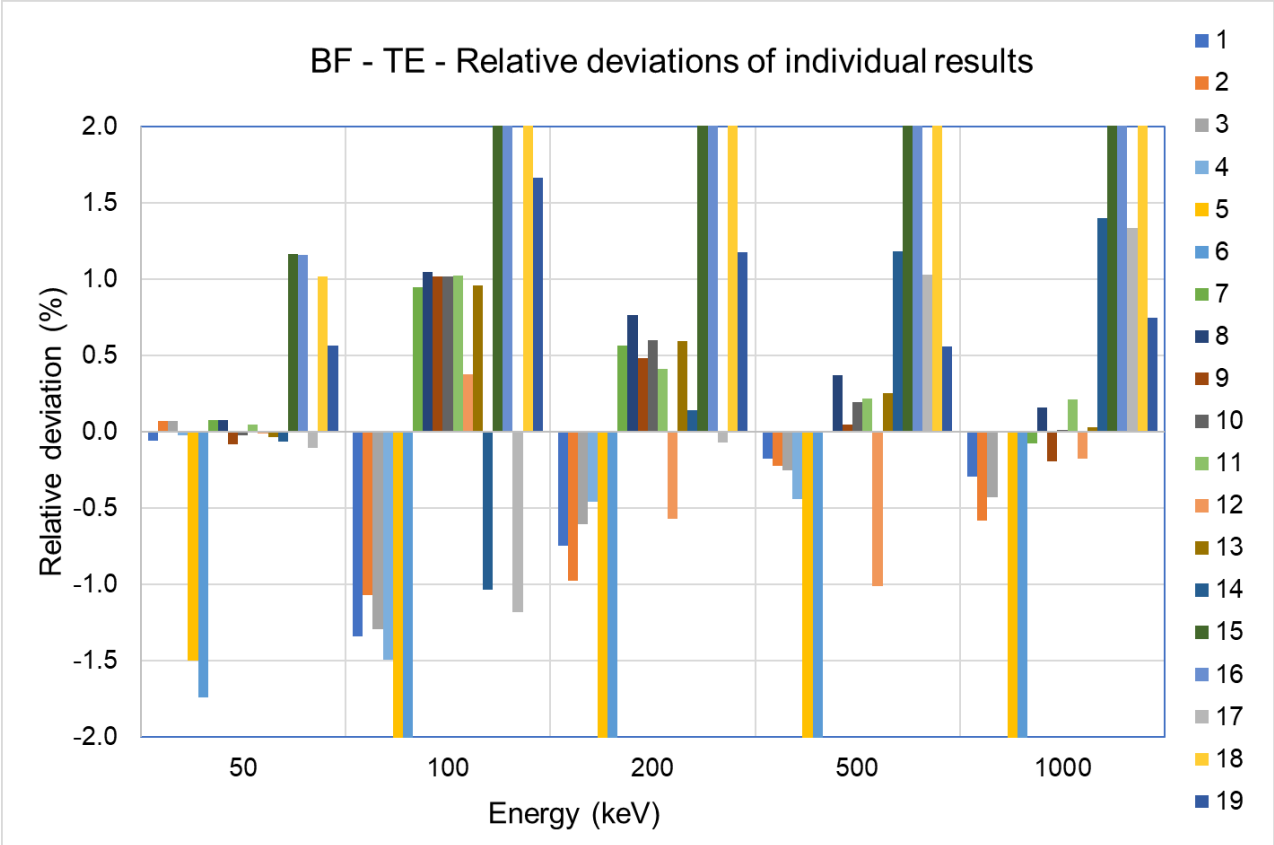
BF - TE - Relative deviations of individual results
Relative deviation (%)
2.0
1.5
1.0
0.5
0.0
-0.5
-1.0
-1.5
-2.0
50
100
200
500
1000
Energy (keV)
1
2
3
4
5
6
7
8
9
10
11
12
13
14
15
16
17
18
19

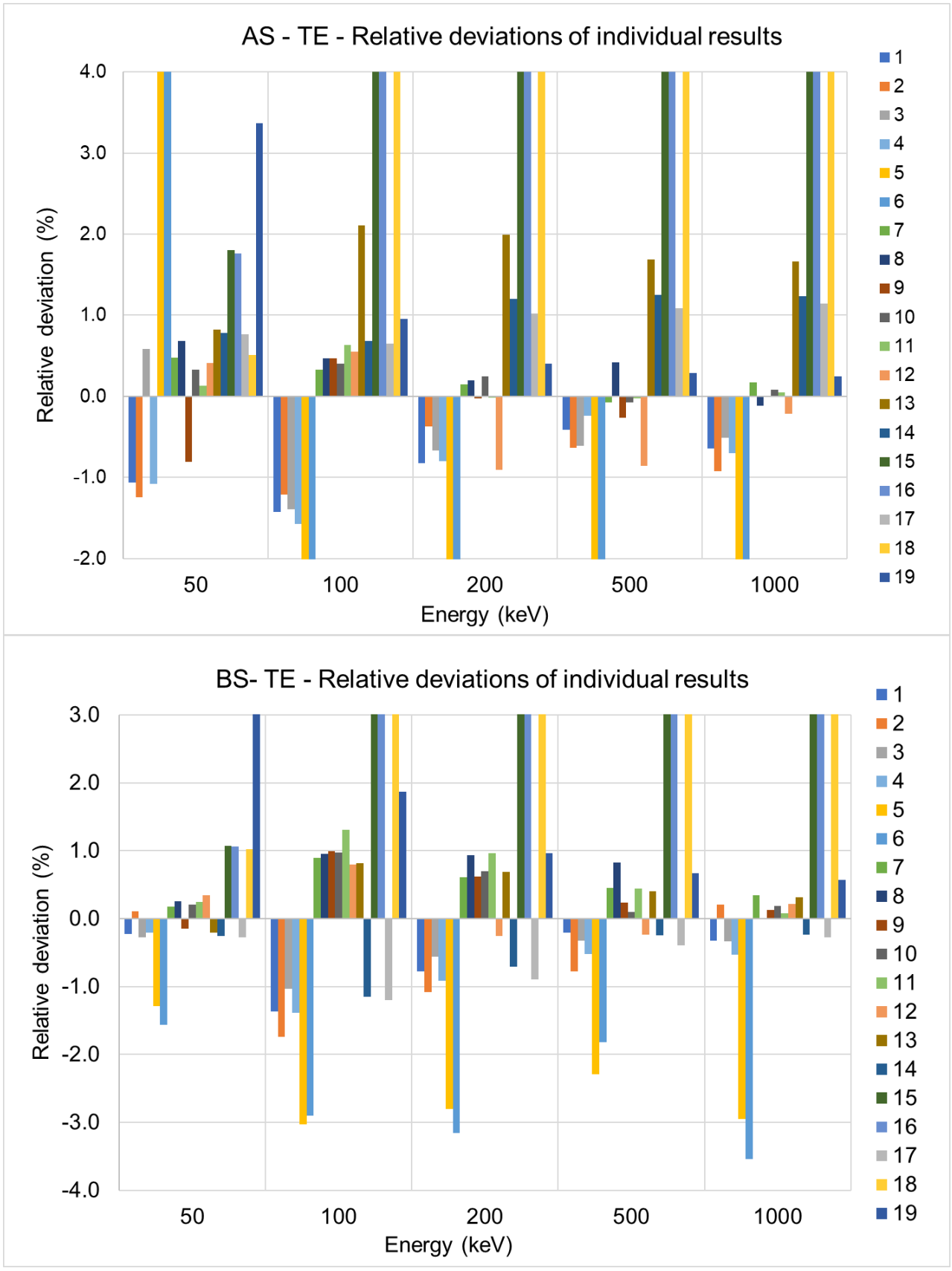

Figure 32 : Deviation of individual results relative to the mean value (%) for the total efficiencies